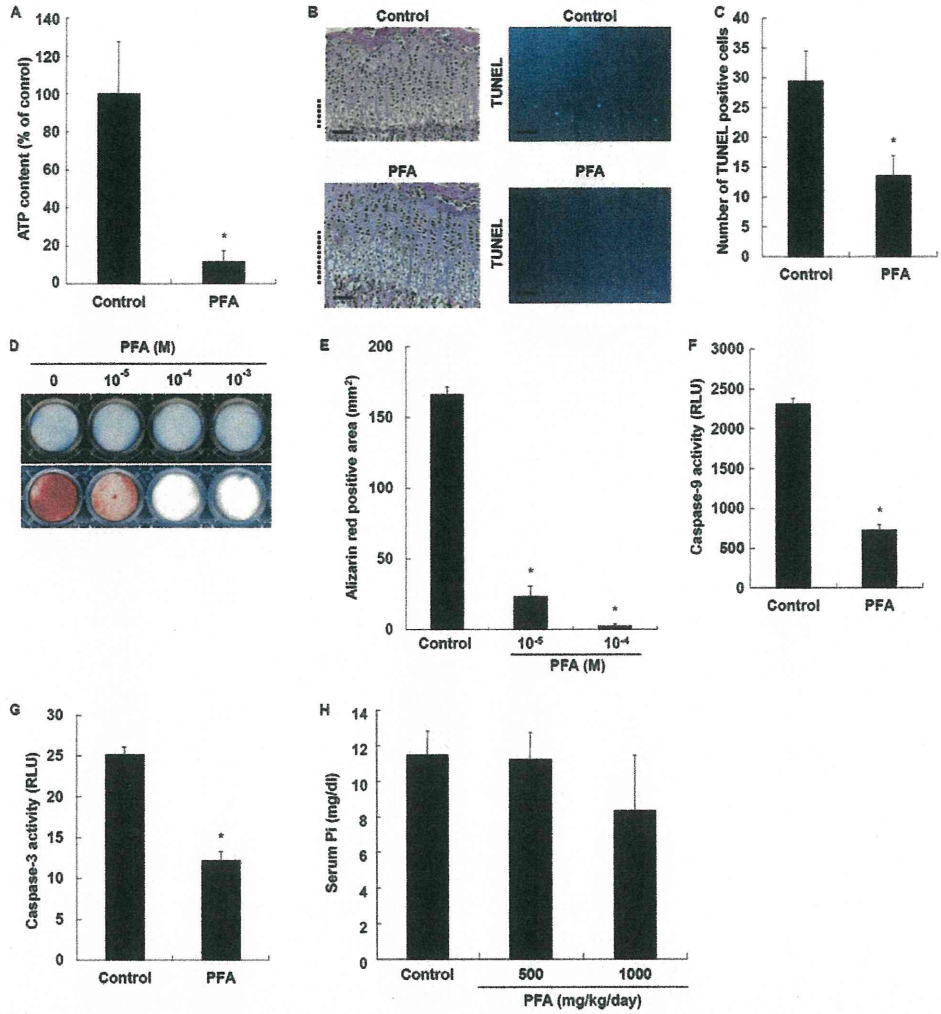

FIGURE 4. **Effects of PFA on chondrocyte differentiation.** *A*, intracellular ATP levels. Cells were cultured in the presence of 10^{-5} M PFA. ATP levels were measured using the ATP assay kit. *B*, histological examination of chondrocyte apoptosis. Hematoxylin/eosin staining (*left*) and TUNEL staining (*right*) were performed on tibial sections from 31-day-old control and PFA-treated mice. The hypertrophic zone is marked with *dotted lines*, and the *scale bars* indicate 200 μm. Representative pictures obtained of numerous sections of four mice from each group are shown. *C*, number of TUNEL-positive cells in the tibial growth plates of control and PFA-treated mice. *D*, histochemical staining of chondrocytes. Cells were cultured in the presence of 10^{-5} M PFA and stained with Alcian blue for GAG synthesis (*upper*) and alizarin red S for mineralization (*lower*). *E*, quantification of alizarin red staining. *F*, caspase-9 activity. *G*, caspase-3 activity. Cells were cultured in the presence of 10^{-5} M PFA. Activity was measured using the Caspase-Glo 9 and Caspase-Glo 3/7 assays. *H*, serum P_i levels. Results are expressed as the mean ± S.E. of four separate determinations. *, significantly different from control ($p < 0.05$). *RLU*, relative light units.

take via *Pit-1* is specifically involved in the regulation of chondrogenesis, including apoptosis and mineralization.

Suppression of Chondrocyte Differentiation by NPT Inhibitor—To verify whether a decrease in P_i uptake due to reduced *Pit-1* expression is responsible for a reduction in ATP levels in *Hyp* chondrocytes, we determined the effects of PFA (foscarnet), which is a competitive inhibitor of P_i uptake via NPT (23), on intracellular ATP levels. PFA (10^{-5} to 10^{-3} M) reduced P_i uptake in chondrocytes in a dose-dependent manner (data not shown). PFA (10^{-5} M) profoundly reduced intracellular ATP levels (Fig. 4*A*). Of note, PFA treatment caused disorganization of growth plate cartilage (Fig. 4*B*, *left*) and significantly decreased the number of TUNEL-positive chondrocytes in hypertrophic cartilage (Fig. 4, *B* (*right*) and *C*) in a similar manner to that seen in *Hyp* mice. Consistent with these *in vivo* results, PFA markedly inhibited mineralization of chondrocytes in a dose-dependent manner (Fig. 4, *D* (*lower*) and *E*), whereas GAG synthesis was not affected by PFA treatment (Fig. 4*D*, *upper*). Furthermore, PFA also inhibited caspase-9 (Fig. 4*F*) and caspase-3 (Fig. 4*G*) activity. We determined serum P_i levels in PFA-treated mice. There was a trend of decreased serum P_i levels in PFA-treated mice, but it was not significantly different (Fig. 4*H*). The results are consistent with the notion that P_i uptake via *Pit-1* is closely associated with late chondrogenesis, including apoptosis and mineralization, through reducing ATP synthesis. These results also suggest an important role for intracellular P_i over extracellular P_i in the regulation of apoptosis and ATP synthesis in chondrocytes.

Suppression of Chondrocyte Differentiation by NPT siRNA—To further and more specifically verify the role of *Pit-1* in chondrocyte differentiation, we performed knockdown experiments using siRNA for *Pit-1*. As control, *Npt2a* was also knocked down. *Pit-1* and *Npt2a* siRNAs profoundly reduced

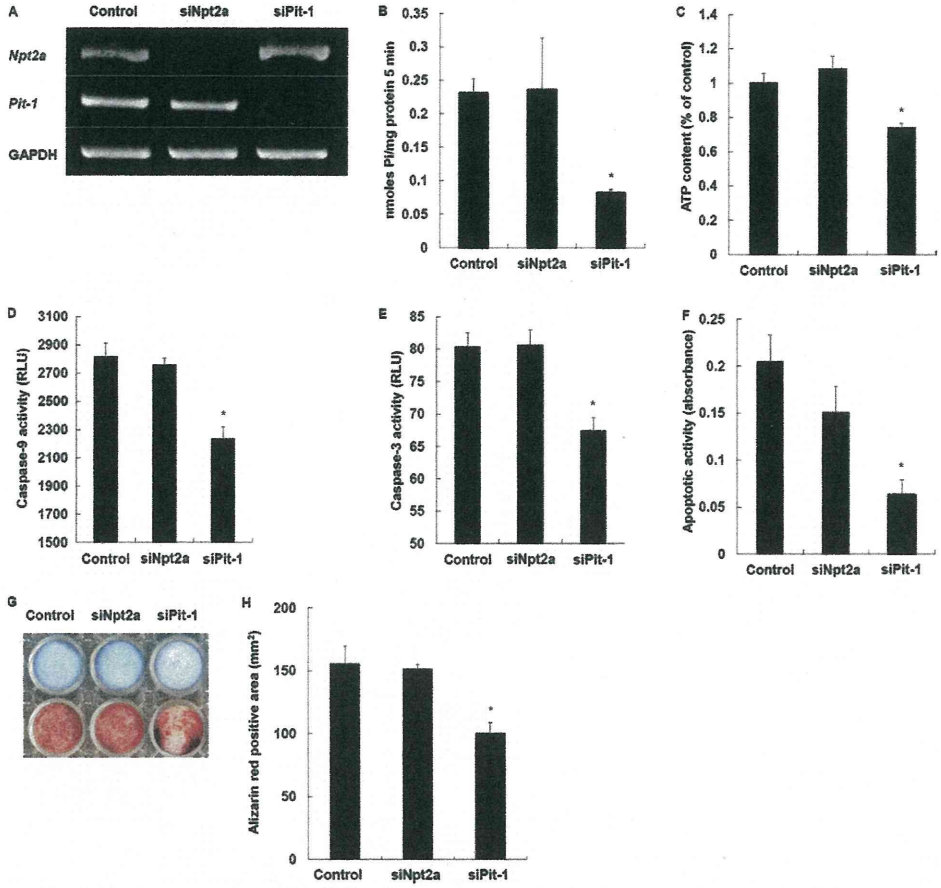

FIGURE 5. ***Npt2a* and *Pit-1* knockdown by siRNA in chondrocytes.** *A*, negative control, *Npt2a*, or *Pit-1* siRNA was transfected in chondrocytes, and the expression of *NPT2a*, *Pit-1*, or GAPDH was analyzed by RT-PCR. *B*, P_i uptake in negative control, *Npt2a* (*siNpt2a*), and *Pit-1* (*siPit-1*) siRNA-transfected chondrocytes was determined in the presence of 3 μCi/ml $KH_2{}^{32}PO_4$. *C*, intracellular ATP levels in negative control, *Npt2a*, and *Pit-1* siRNA-transfected chondrocytes. *D*, caspase-9 activity in negative control, *Npt2a*, and *Pit-1* siRNA-transfected chondrocytes. *E*, caspase-3 activity in negative control, *Npt2a*, and *Pit-1* siRNA-transfected chondrocytes. *F*, quantitative determination of chondrocyte apoptosis in negative control, *Npt2a*, and *Pit-1* siRNA-transfected chondrocytes. *G*, histochemical staining of negative control, *Npt2a*, and *Pit-1* siRNA-transfected chondrocytes. Cells were cultured and stained with Alcian blue for GAG synthesis (*upper*) and alizarin red S for mineralization (*lower*). *H*, quantification of alizarin red staining. We repeated the experiments twice using different preparations of primary chondrocytes and obtained identical results. Results are expressed as the mean ± S.E. of two separate determinations. *, significantly different from control ($p < 0.05$). *RLU*, relative light units.

Pit-1 and *Npt2a* mRNA levels in WT chondrocytes, respectively (Fig. 5*A*). *Pit-1* knockdown by *Pit-1* siRNA significantly decreased P_i uptake (Fig. 5*B*), intracellular ATP levels (Fig. 5*C*), and caspase-9 (Fig. 5*D*) and caspase-3 (Fig. 5*E*) activity. In parallel with these, apoptosis (Fig. 5*F*) and mineralization (Fig. 5, *G* and *H*) were also suppressed. In contrast, knockdown of *Npt2a* by *Npt2a* siRNA had no effects on apoptosis, mineralization, and other determinations (Fig. 5, *B–H*). These data suggest that *Pit-1* specifically controls P_i uptake following cascades of ATP-dependent caspase signaling, apoptosis, and mineralization in chondrocytes.

Recovery of Differentiation in Hyp Chondrocytes by Pit-1 Overexpression—As an alternative approach to confirm a critical role of *Pit-1* in apoptosis and mineralization in chondrocytes, we next examined the effects of *Pit-1* overexpression on *Hyp* chondrocytes. *Pit-1* overexpression significantly increased P_i uptake (Fig. 6*A*) and intracellular ATP levels (Fig. 6*B*) in *Hyp* chondrocytes. Furthermore, *Pit-1* overexpression also stimulated caspase-9 (Fig. 6*C*) and caspase-3 (Fig. 6*D*) activity, apoptosis (Fig. 6*E*), and mineralization (Fig. 6, *F* and *G*). WT chondrocytes also showed significantly increased P_i uptake (Fig. 6*A*), intracellular ATP levels (Fig. 6*B*), caspase-9 (Fig. 6*C*) and caspase-3 (Fig. 6*D*) activity, apoptosis (Fig. 6*E*), and mineralization (Fig. 6, *F* and *G*) by *Pit-1* overexpression. These results further suggest that *Pit-1* is critical in the regulation of P_i uptake and following cascades of ATP-dependent caspase signaling, apoptosis, and mineralization in chondrocytes.

Suppression of Chondrocyte Differentiation by ATP Synthesis Inhibitor—To further examine the role of intracellular ATP in chondrocyte differentiation, we studied the effects of the ATP synthesis inhibitor 3-BrPA. 3-BrPA (10^{-6} M) significantly reduced intracellular ATP levels in WT chondrocytes in culture (data not shown). Caspase-9 (Fig. 7*A*) and caspase-3 (Fig. 7*B*) activity was also significantly decreased in 3-BrPA-treated chondrocytes. More importantly, 3-BrPA treatment significantly decreased the number of TUNEL-positive chondrocytes in the hypertrophic zone in mice (Fig. 7, *C* and *D*). 3-BrPA inhibited chondrocyte mineralization in a dose-dependent manner (Fig. 7, *E* and *F*). However, GAG synthesis was not affected by 3-BrPA (Fig. 7*E*). The serum P_i levels in 3-BrPA-treated mice were not significantly different from those in control mice (Fig. 7*G*), suggesting an important role

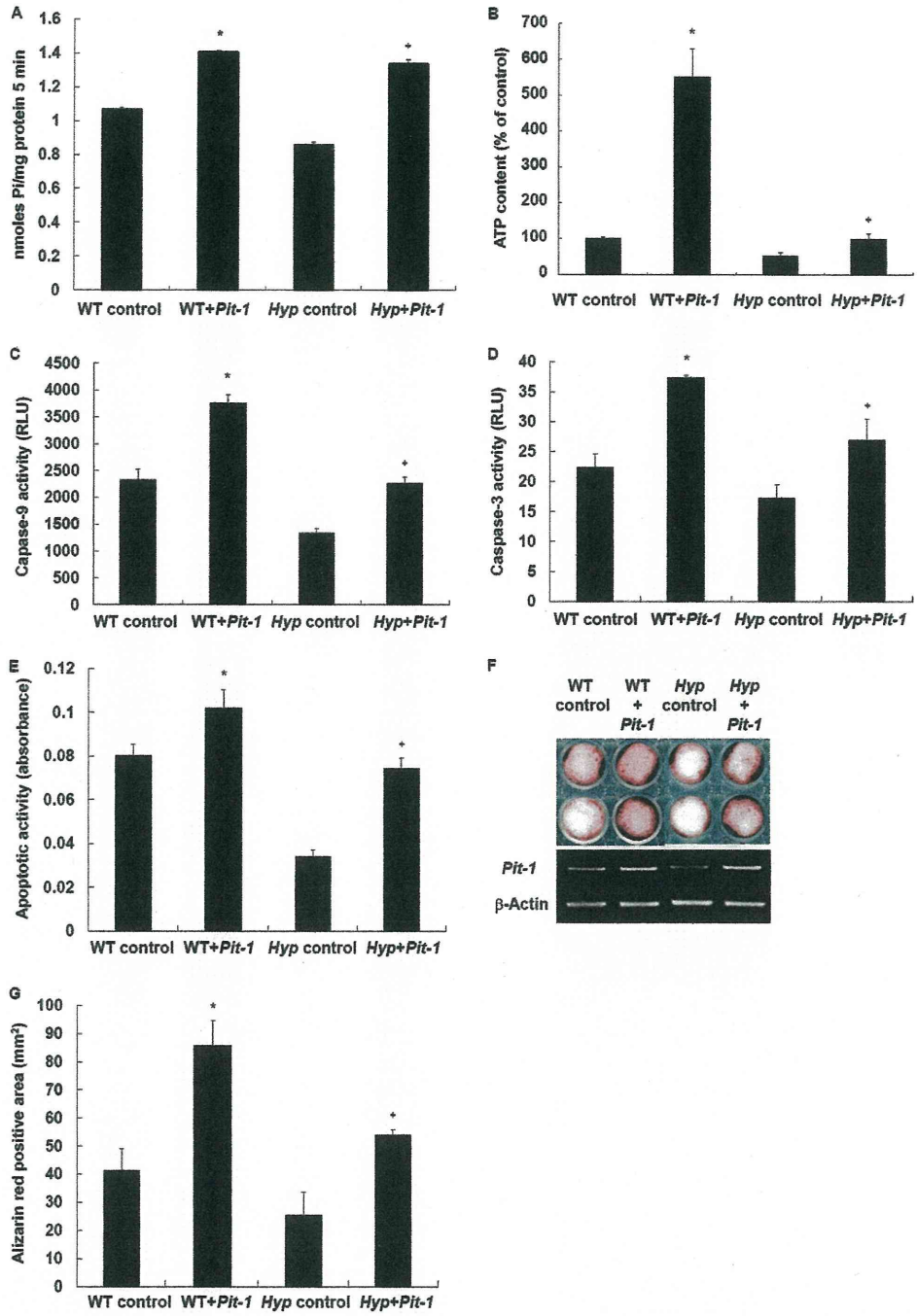

FIGURE 6. **Effects of *Pit-1* overexpression in chondrocytes.** *A*, empty vector (control) or *Pit-1* was transfected in WT and *Hyp* chondrocytes. P_i uptake was determined in the presence of 3 μCi/ml $KH_2{}^{32}PO_4$. *B*, intracellular ATP levels in control or *Pit-1*-transfected WT and *Hyp* chondrocytes. *C*, caspase-9 activity in control and *Pit-1*-transfected WT and *Hyp* chondrocytes. *D*, caspase-3 activity in control and *Pit-1*-transfected WT and *Hyp* chondrocytes. *E*, quantitative determination of apoptosis in control and *Pit-1*-transfected WT and *Hyp* chondrocytes. *F*, histochemical staining of control and *Pit-1*-transfected WT and *Hyp* chondrocytes. Cells were cultured and stained with alizarin red S for mineralization. *Pit-1* expression was confirmed by RT-PCR. *G*, quantification of alizarin red staining. We repeated the experiments twice using different preparations of primary chondrocytes and obtained identical results. Results are expressed as the mean ± S.E. of two separate determinations. *, significantly different from WT control ($p < 0.05$). +, significantly different from *Hyp* control ($p < 0.05$). *RLU*, relative light units.

for intracellular P_i over extracellular P_i. These results suggest that ATP synthesis is important for chondrocytes to undergo apoptosis via caspase signaling and advance to mineralization.

DISCUSSION

In this study, we explored the role of the P_i-NPT system in chondrogenesis using *Hyp* mice compared with WT mice. We found that *Hyp* mice exhibited a widened and disorganized hypertrophic zone with reduced chondrocyte apoptosis compared with WT mice. In addition, PFA (a competitive inhibitor of *Pit-1*) or 3-BrPA (an ATP synthesis inhibitor) markedly caused elongation and disorganization of hypertrophic cartilage with reduced apoptosis in WT mice in a similar manner to that in *Hyp* mice. It is noted that the disorders in the hy-

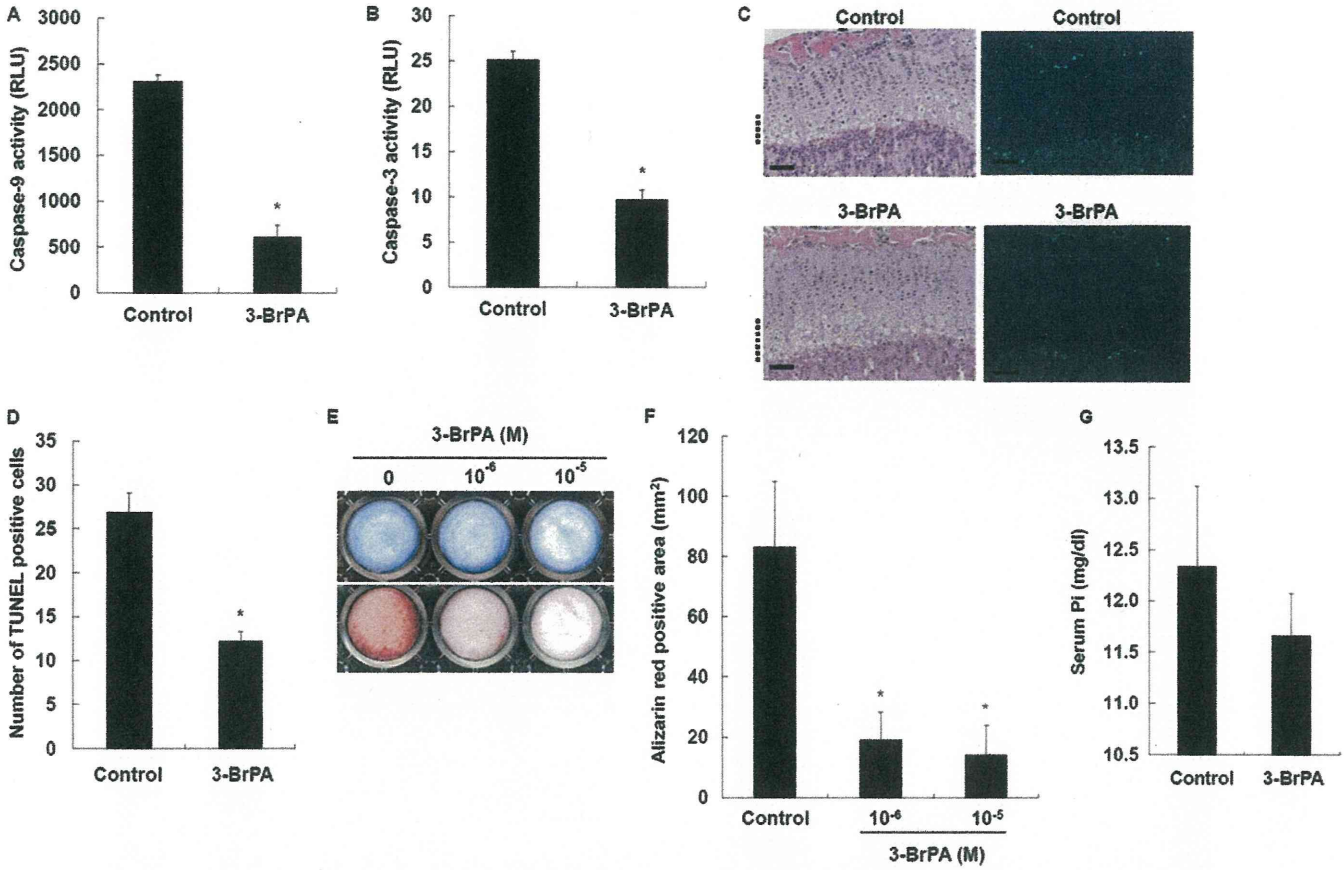

FIGURE 7. **Effects of 3-BrPA on chondrocyte apoptosis and calcification.** *A*, effects of 3-BrPA on caspase-9 activity. *B*, effects of 3-BrPA on caspase-3 activity. Cells were treated with 10^{-6} M 3-BrPA for 7 days and measured for caspase activity. *C*, histological examination of chondrocyte apoptosis. Hematoxylin/eosin staining (*left*) and TUNEL staining (*right*) were performed on tibial sections from 31-day-old control and 3-BrPA-treated mice. The hypertrophic zone is marked with *dotted lines*, and the *scale bars* indicate 200 μm. *D*, number of TUNEL-positive cells in tibial growth plates of control and 3-BrPA-treated mice. *E*, histochemical staining of chondrocytes. Cells were cultured for 7 days in the presence of 10^{-6} and 10^{-5} M 3-BrPA, and stained with Alcian blue for GAG synthesis (*upper*) and alizarin red S for mineralization (*lower*). *F*, quantification of alizarin red staining. *G*, serum P_i levels. Results are expressed as the mean ± S.E. of four separate experiments. *, significantly different from control ($p < 0.05$). *RLU*, relative light units.

pertrophic zone were most severe in *Hyp* mice compared with PFA- or 3-BrPA-treated mice, despite the fact that the number of TUNEL-positive cells are comparable in these mice. We postulate that the disorders in *Hyp* mice are congenital and irreversible and thus most severe, whereas the disorders seen in PFA- and 3-BrPA-treated mice are due to transient exposure of these agents and reversible and thus less severe.

Consistent with these *in vivo* results, *Hyp* chondrocytes in culture exhibited decreased activity of apoptotic signaling, including caspase-9 and caspase-3, apoptosis, and mineralization following reduced P_i uptake and cellular ATP synthesis. Furthermore, PFA or 3-BrPA diminished caspase-9 and caspase-3 activity, apoptosis, and mineralization in conjunction with a reduction in P_i uptake and ATP synthesis in WT chondrocytes. *Hyp* primary chondrocytes displayed a decrease in *Pit-1* (type III NPT) mRNA expression compared with WT chondrocytes, whereas there was no difference in type IIa NPT mRNA expression between WT and *Hyp* chondrocytes. WT and *Hyp* chondrocytes expressed no type I NPT mRNA. Meanwhile, GAG synthesis, which is an early event in chondrogenesis, was not reduced in *Hyp* chondrocytes, and PFA and 3-BrPA knockdown of *Pit-1* failed to decrease GAG synthesis in WT chondrocytes. *Pit-1* overexpression restored apoptosis and mineralization in *Hyp* chondrocytes. Taken together, these results suggest that P_i uptake via *Pit-1* and consequent ATP synthesis are critical in the regulation of late chondrogenesis, including apoptosis and mineralization. These results also suggest that the disruption of cellular P_i homeostasis causes abnormal endochondral ossification due to a reduction of ATP synthesis in Hyp mice. In support of our study, Zalutskaya *et al.* (32) have recently described that P_i activates mitochondrial apoptotic pathways and promotes endochondral ossification.

ATP Synthesis and Chondrogenesis—A notable and novel finding obtained in this study is that 3-BrPA inhibits apoptosis and mineralization in growth plate hypertrophic cartilage *in vivo* and primary chondrocytes *in vitro*. 3-BrPA is an alkylating agent that decreases cellular ATP via inhibition of hexokinase in glycolysis and has been shown to promote cancer cell death through activation of the mitochondrial pathway of apoptosis or necrosis (33). Of note, the ATP-depleting effect of 3-BrPA is prominent only in tumor cells but is not apparent in nontransformed cells (34). Hence, it has been proposed that 3-BrPA could be an anticancer agent for a variety of cancers. In addition to these effects on cancers, our results show that 3-BrPA inhibits the differentiation of cartilage, suggest-

ing that ATP generation is also necessary for nontransformed chondrocytes to differentiate and that chondrogenesis is thus an energy-dependent biological event.

Decreased Pit-1 Expression and Hyp Skeletal Phenotype—Decreased P_i uptake in *Hyp* chondrocytes is likely primarily due to reduced *Pit-1* mRNA expression. Type IIa NPT expression was not diminished in *Hyp* chondrocytes, and type I NPT was not expressed in chondrocytes. Earlier reports described that disturbed endochondral ossification was not rescued by P_i supplementation in *Hyp* mice (35–37), suggesting that intrinsic factors are involved. Miao *et al.* (5) showed that reduced expression of *PHEX* and MMP-9 is associated with cartilage abnormalities in *Hyp* mice. Our results suggest that *Pit-1* is one of these intrinsic factors responsible for the abnormal chondrogenesis seen in *Hyp* mice as well.

Regulation of Pit-1 Expression—The mechanism underlying down-regulation of *Pit-1* expression in *Hyp* chondrocytes is unknown. Recent studies have reported that stanniocalcin (STC) 1 increases *Pit-1* mRNA expression in osteoblasts (38), and STC1 and STC2 have been shown to regulate P_i uptake in chicken chondrocytes (39). STC1 stimulates renal P_i uptake and increases *Pit-1* expression in osteoblasts (40), whereas STC2 inhibits *Pit-1* expression and renal P_i uptake (38). Thus, STC1 and STC2 have an opposite action in the regulation of *Pit-1* expression. Therefore, it is intriguing to examine whether STC1 or STC2 is involved in *Pit-1* expression in chondrocytes. In preliminary experiments, we determined the expression of STC1 and STC2 mRNAs in WT and *Hyp* chondrocytes using RT-PCR and real-time PCR. The STC2 mRNA was expressed in both WT and *Hyp* chondrocytes at the same level (data not shown). However, the expression of STC1 mRNA was decreased in *Hyp* chondrocytes compared with WT chondrocytes (data not shown). These results suggest that STC1, but not STC2, regulates *Pit-1* expression in chondrocytes.

Involvement of FGF23—FGF23 (fibroblast growth factor 23) is a hormone that regulates serum P_i levels (41). FGF23 requires Klotho for its signaling as the coreceptor in addition to the canonical FGFR1(IIIc) (42, 43). Mice transgenic for FGF23 display a reduction in *Npt2a* expression in the renal proximal tubules (44), indicating that FGF23 is a negative regulator of *Npt2a* expression, raising the possibility that Klotho-dependent FGF23 signaling regulates *Pit-1* expression in chondrocytes as well. FGF23 expression is localized predominantly in osteoblasts, cementoblasts, and odontoblasts, with a sporadic expression in some chondrocytes, osteocytes, and cementocytes (45). However, we were not able to demonstrate FGF23 expression in primary mouse chondrocytes by RT-PCR. Further studies are needed to elucidate the relationship between FGF23 signaling and *Pit-1* expression in cartilage.

In conclusion, we have found in this study that chondrogenesis is modulated by cellular P_i uptake via *Pit-1* and cellular ATP synthesis and thus is a biological event that depends on mitochondrial energy generation. We believe that these findings should provide us with a novel concept and alternative approaches to study the cellular differentiation that occurs in physiological conditions and also to analyze the skeletal abnormalities seen in congenital hypophosphatemic disorders such as XLH.

Acknowledgments—We thank Drs. Kenichi Miyamoto and Hiroko Segawa (University of Tokushima Graduate School, Tokushima, Japan) for the kind gift of mouse Pit-1 cDNA.

REFERENCES

1. Zuscik, M. J., Hilton, M. J., Zhang, X., Chen, D., and O'Keefe, R. J. (2008) *J. Clin. Invest.* **118,** 429–438
2. Winters, R. W., Graham, J. B., Williams, T. F., McFalls, V. W., and Burnett, C. H. (1958) *Medicine* **37,** 97–142
3. Holm, I. A., Huang, X., and Kunkel, L. M. (1997) *Am. J. Hum. Genet.* **60,** 790–797
4. Eicher, E. M., Southard, J. L., Scriver, C. R., and Glorieux, F. H. (1976) *Proc. Natl. Acad. Sci. U.S.A.* **73,** 4667–4671
5. Miao, D., Bai, X., Panda, D. K., Karaplis, A. C., Goltzman, D., and McKee, M. D. (2004) *Bone* **34,** 638–647
6. Hayashibara, T., Hiraga, T., Sugita, A., Wang, L., Hata, K., Ooshima, T., and Yoneda, T. (2007) *J. Bone Miner. Res.* **22,** 1743–1751
7. Boyde, A., and Shapiro, I. M. (1980) *Histochemistry* **69,** 85–94
8. Kakuta, S., Golub, E. E., and Shapiro, I. M. (1985) *Calcif. Tissue Int.* **37,** 293–299
9. Mwale, F., Tchetina, E., Wu, C. W., and Poole, A. R. (2002) *J. Bone Miner. Res.* **17,** 275–283
10. Shapiro, I. M., and Boyde, A. (1984) *Metab. Bone Dis. Relat. Res.* **5,** 317–326
11. Virkki, L. V., Biber, J., Murer, H., and Forster, I. C. (2007) *Am. J. Physiol. Renal. Physiol.* **293,** F643–F654
12. Palmer, G., Zhao, J., Bonjour, J., Hofstetter, W., and Caverzasio, J. (1999) *Bone* **24,** 1–7
13. Mansfield, K., Teixeira, C. C., Adams, C. S., and Shapiro, I. M. (2001) *Bone* **28,** 1–8
14. Cecil, D. L., Rose, D. M., Terkeltaub, R., and Liu-Bryan, R. (2005) *Arthritis Rheum.* **52,** 144–154
15. Fujita, T., Meguro, T., Izumo, N., Yasutomi, C., Fukuyama, R., Nakamuta, H., and Koida, M. (2001) *Jpn. J. Pharmacol.* **85,** 278–281
16. Guicheux, J., Palmer, G., Shukunami, C., Hiraki, Y., Bonjour, J. P., and Caverzasio, J. (2000) *Bone* **27,** 69–74
17. Montessuit, C., Caverzasio, J., and Bonjour, J. P. (1991) *J. Biol. Chem.* **266,** 17791–17797
18. Wang, D., Canaff, L., Davidson, D., Corluka, A., Liu, H., Hendy, G. N., and Henderson, J. E. (2001) *J. Biol. Chem.* **276,** 33995–34005
19. Wu, L. N., Guo, Y., Genge, B. R., Ishikawa, Y., and Wuthier, R. E. (2002) *J. Cell. Biochem.* **86,** 475–489
20. Magne, D., Bluteau, G., Faucheux, C., Palmer, G., Vignes-Colombeix, C., Pilet, P., Rouillon, T., Caverzasio, J., Weiss, P., Daculsi, G., and Guicheux, J. (2003) *J. Bone Miner. Res.* **18,** 1430–1442
21. Shimomura, Y., Yoneda, T., and Suzuki, F. (1975) *Calcif. Tissue Res.* **19,** 179–187
22. Rowe, P. S., Ong, A. C., Cockerill, F. J., Goulding, J. N., and Hewison, M. (1996) *Bone* **18,** 159–169
23. Loghman-Adham, M. (1996) *Gen. Pharmacol.* **27,** 305–312
24. Swenson, C. L., Weisbrode, S. E., Nagode, L. A., Hayes, K. A., Steinmeyer, C. L., and Mathes, L. E. (1991) *Calcif. Tissue Int.* **48,** 353–361
25. Geschwind, J. F., Ko, Y. H., Torbenson, M. S., Magee, C., and Pedersen, P. L. (2002) *Cancer Res.* **62,** 3909–3913
26. Jones, A. R., Gillan, L., and Milmlow, D. (1995) *Contraception* **52,** 317–320
27. Ko, Y. H., Smith, B. L., Wang, Y., Pomper, M. G., Rini, D. A., Torbenson, M. S., Hullihen, J., and Pedersen, P. L. (2004) *Biochem. Biophys. Res. Commun.* **324,** 269–275
28. Gibson, G. (1998) *Microsc. Res. Tech.* **43,** 191–204
29. Eguchi, Y., Srinivasan, A., Tomaselli, K. J., Shimizu, S., and Tsujimoto, Y. (1999) *Cancer Res.* **59,** 2174–2181
30. Li, P., Nijhawan, D., Budihardjo, I., Srinivasula, S. M., Ahmad, M., Al-

nemri, E. S., and Wang, X. (1997) *Cell* **91,** 479–489
31. Rao, N. N., Gómez-García, M. R., and Kornberg, A. (2009) *Annu. Rev. Biochem.* **78,** 605–647
32. Zalutskaya, A. A., Cox, M. K., and Demay, M. B. (2009) *J. Cell. Biochem.* **108,** 668–674
33. Pelicano, H., Martin, D. S., Xu, R. H., and Huang, P. (2006) *Oncogene* **25,** 4633–4646
34. Xu, R. H., Pelicano, H., Zhou, Y., Carew, J. S., Feng, L., Bhalla, K. N., Keating, M. J., and Huang, P. (2005) *Cancer Res.* **65,** 613–621
35. Ecarot, B., Glorieux, F. H., Desbarats, M., Travers, R., and Labelle, L. (1992) *J. Bone Miner. Res.* **7,** 523–530
36. Tanaka, H., Seino, Y., Shima, M., Yamaoka, K., Yabuuchi, H., Yoshikawa, H., Masuhara, K., Takaoka, K., and Ono, K. (1988) *Bone Miner.* **4,** 237–246
37. Yoshikawa, H., Masuhara, K., Takaoka, K., Ono, K., Tanaka, H., and Seino, Y. (1985) *Bone* **6,** 235–239
38. Yoshiko, Y., Candeliere, G. A., Maéda, N., and Aubin, J. E. (2007) *Mol. Cell. Biol.* **27,** 4465–4474
39. Wu, S., Yoshiko, Y., and De Luca, F. (2006) *J. Biol. Chem.* **281,** 5120–5127
40. Ishibashi, K., and Imai, M. (2002) *Am. J. Physiol. Renal Physiol.* **282,** F367–F375
41. Fukumoto, S., and Yamashita, T. (2007) *Bone* **40,** 1190–1195
42. Kurosu, H., Ogawa, Y., Miyoshi, M., Yamamoto, M., Nandi, A., Rosenblatt, K. P., Baum, M. G., Schiavi, S., Hu, M. C., Moe, O. W., and Kuro-o, M. (2006) *J. Biol. Chem.* **281,** 6120–6123
43. Urakawa, I., Yamazaki, Y., Shimada, T., Iijima, K., Hasegawa, H., Okawa, K., Fujita, T., Fukumoto, S., and Yamashita, T. (2006) *Nature* **444,** 770–774
44. Shimada, T., Urakawa, I., Yamazaki, Y., Hasegawa, H., Hino, R., Yoneya, T., Takeuchi, Y., Fujita, T., Fukumoto, S., and Yamashita, T. (2004) *Biochem. Biophys. Res. Commun.* **314,** 409–414
45. Yoshiko, Y., Wang, H., Minamizaki, T., Ijuin, C., Yamamoto, R., Suemune, S., Kozai, K., Tanne, K., Aubin, J. E., and Maeda, N. (2007) *Bone* **40,** 1565–1573

OPEN ACCESS Freely available online

PLoS one

P38 Mitogen-Activated Protein Kinase Inhibitor, FR167653, Inhibits Parathyroid Hormone Related Protein-Induced Osteoclastogenesis and Bone Resorption

Huiren Tao[1,2☯], Mina Okamoto[1☯], Masataka Nishikawa[1], Hideki Yoshikawa[1], Akira Myoui[1]*

1 Department of Orthopedics, Osaka University Graduate School of Medicine, Osaka, Japan, **2** Department of Orthopedics, Xijing Hospital, Fourth Military Medical University, Xi'an, China

Abstract

p38 mitogen-activated protein kinase (MAPK) acts downstream in the signaling pathway that includes receptor activator of NF-κB (RANK), a powerful inducer of osteoclast formation and activation. We investigated the role of p38 MAPK in parathyroid hormone related protein (PTHrP)-induced osteoclastogenesis *in vitro* and PTHrP-induced bone resorption *in vivo*. The ability of FR167653 to inhibit osteoclast formation was evaluated by counting the number of tartrate-resistant acid phosphatase positive multinucleated cells (TRAP-positive MNCs) in *in vitro* osteoclastgenesis assays. Its mechanisms were evaluated by detecting the expression level of c-Fos and nuclear factor of activated T cells c1 (NFATc1) in bone marrow macrophages(BMMs) stimulated with sRANKL and M-CSF, and by detecting the expression level of osteoprotegerin (OPG) and RANKL in bone marrow stromal cells stimulated with PTHrP in the presence of FR167653. The function of FR167653 on bone resorption was assessed by measuring the bone resorption area radiographically and by counting osteoclast number per unit bone tissue area in calvaria in a mouse model of bone resorption by injecting PTHrP subcutaneously onto calvaria. Whole blood ionized calcium levels were also recorded. FR167653 inhibited PTHrP-induced osteoclast formation and PTHrP-induced c-Fos and NFATc1 expression in bone marrow macrophages, but not the expression levels of RANKL and OPG in primary bone marrow stromal cells treated by PTHrP. Furthermore, bone resorption area and osteoclast number in vivo were significantly decreased by the treatment of FR167653. Systemic hypercalcemia was also partially inhibited. Inhibition of p38 MAPK by FR167653 blocks PTHrP-induced osteoclastogenesis *in vitro* and PTHrP-induced bone resorption *in vivo*, suggesting that the p38 MAPK signaling pathway plays a fundamental role in PTHrP-induced osteoclastic bone resorption.

Citation: Tao H, Okamoto M, Nishikawa M, Yoshikawa H, Myoui A (2011) P38 Mitogen-Activated Protein Kinase Inhibitor, FR167653, Inhibits Parathyroid Hormone Related Protein-Induced Osteoclastogenesis and Bone Resorption. PLoS ONE 6(8): e23199. doi:10.1371/journal.pone.0023199

Editor: Harish Pant, National Institutes of Health, United States of America

Received June 7, 2011; **Accepted** July 8, 2011; **Published** August 23, 2011

Funding: This work was supported by grants from the Ministry of Education, Culture, Sports, Science and Technology, Japan and by the Ministry of Health, Labor and Welfare, Japan. The funders had no role in study design, data collection and analysis, decision to publish, or preparation of the manuscript.

Competing Interests: The authors have declared that no competing interests exist.

* E-mail: myoi@hp-mctr.med.osaka-u.ac.jp

☯ These authors contributed equally to this work.

Introduction

Parathyroid hormone related protein (PTHrP), a potent stimulator of osteoclastic bone resorption, was first identified as a causative factor for humoral hypercalcemia of malignancy [1]. A number of clinicopathological and experimental studies have shown that cancer cell-derived PTHrP promotes osteoclastic bone resorption and contributes to the development and progression of cancer metastasis to bone [2–5]. PTHrP stimulates osteoclastogenesis by acting on osteoblasts and/or bone marrow stromal cells to increase receptor activator of NF-κB ligand (RANKL) expression and reduce osteoprotegerin (OPG) expression, not by acting directly on osteoclast precursors [6]. Osteoclast precursors that express RANK, a tumor necrosis factor (TNF) receptor family member, recognize RANKL and differentiate into osteoclasts in the presence of macrophage/monocyte colony stimulating factor (M-CSF). OPG is a soluble decoy receptor for RANKL and has the ability to inhibit osteoclastogenesis. Therefore, a relative increase of RANKL versus OPG expression by PTHrP activates osteoclastic bone resorption [7–12].

Additionally, a body of evidence suggested that p38 mitogen-activated protein kinase (MAPK) is downstream of the RANK signaling pathway and plays an important role in osteoclast differentiation. The expression of dominant-negative forms of p38 MAPK in RAW264.7 cells inhibited RANKL-induced differentiation of these cells into osteoclasts [13]. Li et al used pyridinylimidazole SB203580, a specific inhibitor of p38 MAPK, to study p38 MAPK function and demonstrated that p38 MAPK is required for osteoclast differentiation [14].

FR167653 was first discovered as a potent inhibitor of TNFα and interleukin (IL)-1β production in lipopolysaccharide-stimulated human monocytes and phytohemagglutinin-M-stimulated human lymphocytes [15,16]. FR167653 inhibits the activation of p38 MAPK by suppressing the phosphorylation of p38 MAPK, preferentially affecting its α isoform, but not the γ isoform [17–19]. FR167653 is effective in treating inflammation, relieving trauma

and ischemia-reperfusion injury *in vivo* [20–22]. We previously reported that M-CSF-dependent sRANKL- and TNFα-induced osteoclast formation in primary bone marrow cells, and collagen-induced arthritis in rats were inhibited by FR167653 [23]. However, the relationship of p38 MAPK and PTHrP in osteoclastogenesis and bone resorption is still unclear.

Here we investigate the role of FR167653 on PTHrP-induced osteoclastogenesis, local bone resorption, and hypercalcemia. We found that FR167653 not only blocked osteoclast differentiation induced both by PTHrP and sRANKL with down regulation of c-Fos and NFATc1 in bone marrow macrophages without affecting RANKL and OPG expression in bone marrow stromal cells, but also alleviated bone resorption induced by PTHrP with partial reduction of hypercalcemia in vivo.

Materials and Methods

Animal and reagents

All animal experiments in this study strictly followed a protocol approved by the Institutional Animal Care and Use Committee of Osaka University (approval number: 338). Six-week-old male ddy mice and four- to eight-week-old male BDF1 mice were purchased from Japan SLC (Hamamatsu, Japan) and Oriental Yeast (Tokyo, Japan), respectively. Human recombinant PTHrP (1–34) was purchased from Peptide Institute (Osaka, Japan). M-CSF and soluble recombinant RANKL were purchased from PeproTeck EC (London, UK). FR167653 was provided by Asteras Pharma (Osaka, Japan). c-Fos and actin antibodies were purchased from Cell Signaling Technology (Danvers, USA). NFATc1 antibody was bought from BD Biosciences Pharmingen (Franklin Lakes, USA).

Primary bone marrow cell culture

Bone marrow cells were collected by removing the tibias and femurs from ddy mice and flushing the bone cavity with serum-free alpha-minimum essential medium (αMEM; Invitrogen, Carlsbad, CA). A sample of 7.5×10^5 cells in a volume of 0.5 ml/well were cultured in αMEM supplemented with 10% fetal bovine serum (FBS; Equitech-Bio, Kerrville, TX) in the presence of PTHrP (45 ng/ml). Some cultures received an additional treatment of 10 μM, 1 μM or 0.1 μM FR167653. The medium was changed every two days, replacing half of the medium with 0.25 ml fresh medium containing 90 ng/ml PTHrP and 20 μM, 2 μM and 0.2 μM FR167653. After six days of culture, adherent cells were stained for tartrate-resistant acid phosphatase (TRAP), an osteoclast marker enzyme, using a TRAP staining kit (Hokudo, Sapporo, Japan). TRAP-positive multinucleated cells (MNCs) with three or more nuclei were counted as osteoclasts.

M-CSF-dependent bone marrow macrophage (MDBMMs) culture

M-CSF-dependent bone marrow macrophages (MDBMMs) were cultured as described previously [23–25]. Briefly, bone marrow cells (5×10^6) were cultured in the αMEM supplemented with 10% FBS, and M-CSF at the concentration of 100 ng/ml in 100 mm dishes for three days. Then the cells were washed and harvested with 0.02% ethylene diamine tetra-acetate (EDTA) in phosphate-buffered saline, and seeded at a density of 3×10^5 into 100-mm culture dishes in the presence of M-CSF (100 ng/ml). After three more days of culture, the adherent cells were considered as MDBMMs.

For osteoclast culture, MDBMMs were digested with 0.25% Trypsin-EDTA (Invitrogen) and 1×10^4/well cells were re-plated into 48-well plates in the presence of sRANKL (100 ng/ml) and M-CSF (100 ng/ml). Some cultures were treated with FR167653. After five more days of culture, adherent cells were fixed and stained for TRAP. TRAP-positive MNCs containing three or more nuclei were counted as osteoclasts.

For the detection of the c-Fos and NFATc1expression, MDBMMs were treated by each concentration of FR167653 for 1 hour. Then, sRANKL and M-CSF were added. After another 24 or 48 hour culture, the cells were collected for RNA extraction and protein extraction.

Real-time polymerase chain reaction

Total RNA was extracted from bone marrow cells (for genes of OPG and RANKL) or bone marrow macrophages (for genes of c-fos and NFATc1) by using the RNeasy Mini Kit (Qiagen, Valencia, CA). RNase-free DNase Set (Qiagen) was used to remove the residual DNA. Five micrograms of RNA were reverse transcribed into cDNA with Ready-To-Go You-Prime First-Strand Beads (Amersham Bioscience, Piscataway, NJ). In order to reduce pipetting error, the final volume of cDNA was reached by adding four volumes RNase-free distilled water to the original cDNA. The resultant product was subjected to real-time PCR.

Real-time PCR was performed in a Light Cycler (Roche Applied Science, Indianapolis, IN) with Light cycler-DNA Master SYBR Green I (Roche Applied Science) and were performed according to the standard protocol recommended by the manufacturer. Reverse transcription was followed by 40 cycles of PCR (denaturation at 95°C for 10 min addition of 1-second at 94°C, 5-second annealing at 58, 60, 61, 59 and 58°C for OPG, RANKL, c-fos, NFATc1 and GAPDH, respecticvely, and 10-second extension at 72°C, and each of optimal fluorescence measurement temperature for 1 second as the amplification and quantification programs, 60–99°C with a heating rate of 0.1°C per second as the melting curve program, and finally, cooling to 40°C.

The primer sequences are as follows:

RANKL: sense: 5′-CAC CAT CAG CTG AAG ATA GT-3′

antisense: 5′-CCA AGA TCT CTA ACA TGA CG-3′

OPG: sense: 5′-TGGGACCAAAGTGAATGCC-GAGA-3′

antisense: 5′-AGCTGCTCTGTGGTGAGGTTC-3′

c-fos: sense: 5′-CTGGTGCAGCCCACTCTGGT-3′

antisense: 5′- CTTTCAGCAGATTGGCAATC-3′

NFATc1: sense: 5′- CAACGCCCTGACCACCGATA-3′

antisense: 5′- GGCTGCCTTCCGTCTCATAG-3′

GAPDH: sense: 5′-ACCACAGTCCATGCCATCAC-3′

antisense: 5′- TCCACCACCCTGTTGCTGTA-3′

Semiquantitative RANKL, OPG, c-fos and NFATc1 expression levels were determined by normalizing with GAPDH expression level.

Western blotting

Cells were washed twice with ice-cold PBS and lysed with a buffer containing 20 mM Tris–HCl, 150 mM NaCl, 1% riton X-100, and inhibitors for proteases and phosphatases [25]. Cell lysates were centrifuged at 10,000 g for 20 min and the supernatants were collected. Twenty micrograms of cellular

proteins was resolved by SDS–PAGE and transferred onto nitrocellulose membranes. Membranes were blocked with 5% skim milk in Tris-buffered saline containing 0.1% Tween 20 for 1 h and incubated overnight at 4°C with primary antibodies. Membranes were washed, incubated with appropriate secondary antibodies conjugated to horseradish peroxidase for 1 h, and developed using a chemiluminescence system. Relative protein expression was calculated from band densities obtained in three experiments using UMax PowerLook 1100 scanner (Taiwan) and TotalLab gel image analysis software (Nonlinear Dynamics, New England, UK).

PTHrP-induced bone resorption in an animal model

Male BDF1 mice aged four weeks were injected daily for five days (from day one to five) with PTHrP (18 μg/day; Figure 1). PTHrP was injected into the subcutaneous tissue over the left side of the calvaria twice daily in a volume of 10 μl as described previously [26,27]. This delivery method produces an exaggerated resorptive response in the calvarial bone, as well as a systemic effect as indicated by hypercalcemia. Animals were housed in an accredited facility and all procedures used in the animal experiments complied with the standards described in the Osaka University Medical School Guidelines for the Care and Use of Laboratory Animal.

Treatment Protocol

All animals were additionally treated with FR167653 or distilled water, injected subcutaneously on the mice back as in the protocol shown in Figure 1. Treatment was initiated two days before PTHrP injection.

Before treatment, 50 μl of whole blood was collected retro-orbitally into heparinized capillary tubes (Radiometer, Copenhagen, Denmark) and basal whole-blood ionized calcium levels were determined with a calcium level analyzer (model ABL505, Radiometer; n = 3 from treatment group and control group, respectively). The treatment group (n = 7) was treated with 30 mg/kg of FR167653 twice daily while the control group (n = 5) was treated with distilled water for seven days (including pretreatment). At day three and five, blood samples were taken three hours after injection of PTHrP retro-orbitally to determine the levels of hypercalcemia. Mice were killed on day six, which was 12 hours after the last injection of PTHrP.

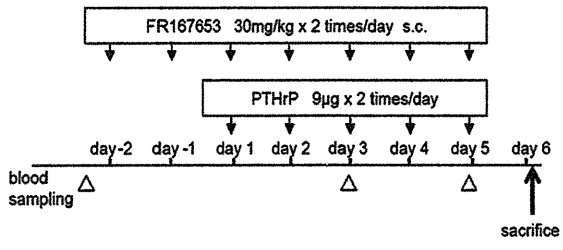

Figure 1. Animal model and treatment protocol. The PTHrP-induced bone resorption animal model was established by injecting PTHrP (18 μg/day) onto the dorsal surface of the mice calvaria daily for five days (day 1 to 5). Animals in the treatment (n = 7) or the control group (n = 5) were injected with FR167653 (30 mg/kg twice daily) or distilled water, respectively, daily for seven days, initiating from two days before PTHrP injection. 50 μl of whole blood was collected retro-orbitally before treatment, on day three, and on day five to determine whole-blood ionized calcium levels. Mice were sacrificed on day six, 12 hours after the last injection of PTHrP.
doi:10.1371/journal.pone.0023199.g001

Quantitative analysis of bone resorption

Calvaria were retrieved from sacrificed mice and immersed into neutral buffered formalin. Radiographs were taken with the MX-20 Specimen Radiography System (Faxitron X-ray, Wheeling, IL). The images were scanned into a computer with a flatbed scanner and saved in RGB color format. The quantitative analysis of calvarial bone resorption was processed with an image analysis software package, WinROOF (Mitani, Fukui, Japan). The thresholds were determined by clicking five typical bone resorptive areas.

After decalcification, the anterior and posterior portions of the calvaria were removed just anterior to coronal suture and posterior to lambdoid suture, respectively. The left part of the calvaria was cut into three strips, embedded in paraffin and sectioned. Sections were stained to detect TRAP activity and counterstained with hematoxylin.

Histomorphormetic analysis was performed on the left side of the calvaria to determine the number of osteoclasts present in the bone. The area measured consisted of six visual fields extending from sagittal suture toward the lateral muscle attachment and included all of the bone and marrow spaces. PTHrP-treated calvaria showed a distinct dorsal periosteal pattern of resorption and endosteal resorption. Thus, the osteoclast number represented the sum of periosteal and endosteal measurements. Results were recorded as osteoclast number per unit bone tissue area measured (OcN-BTA). All measurements were made by tracing the section image onto a digitizing platen with the aid of a cameral lucida attachment and WinROOF image analysis software.

Statistical analysis

All analyses were reported as mean ±S.D. Statistical significance was evaluated by Student's *t*-test or one factor analysis of variance (ANOVA) followed by a Tukey-Kramer post test using a statistical software package, JMP (SAS institute, Cary, NC).

Results

FR167653 inhibits Osteoclast formation in two different cell culture systems

To determine whether FR167653 blocks osteoclastogenesis *in vitro*, we investigated osteoclastogenesis in a primary bone marrow cells stimulated by PTHrP. As expected, TRAP-positive MNCs (osteoclasts) was formed in primary bone marrow cultures treated with PTHrP. As shown in Figure 2, osteoclast formation induced by PTHrP at day six was inhibited by addition of FR167653 in a dose-dependent manner. At the concentration of 10 μM, FR167653 nearly eliminated osteoclast formation.

Unlike bone marrow cells, MDBMM cells are a homogeneous bone marrow macrophage population with a contamination by stromal cells of less than 1 in 1,000 cells. As shown in Figure 3, MDBMM cells formed TRAP-positive osteoclasts when treated with RANKL together with M-CSF even in the absence of stromal cells. FR167653 added to the cultures significantly inhibited RANKL-induced osteoclast formation in a dose-dependent manner. These data suggest that FR167653 acts directly on osteoclast precursors to inhibit osteoclast formation.

OPG and RANKL expression levels in bone marrow cells were not affected by FR167653 treatment

To further elucidate the mechanism of FR167653 inhibition of PTHrP-induced osteoclastogenesis, we examined the effects of FR167653 on the OPG and RANKL expression in bone marrow stromal cells.

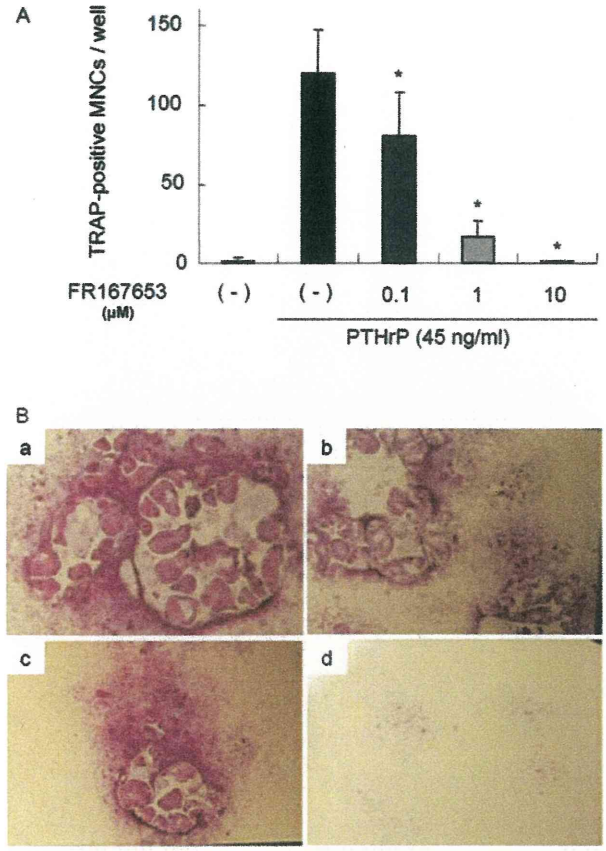

Figure 2. FR167653 inhibits TRAP-positive osteoclast formation in PTHrP-treated bone marrow cells. A. Bone marrow cells were treated with PTHrP (45 ng/ml) and FR167653 for six days. TRAP-positive MNCs with three or more nuclei were counted as osteoclasts. n = 9. *: $p<0.001$ versus the group treated only with PTHrP. B. TRAP staining for bone marrow cells stimulated with PTHrP (45 ng/ml). a: no treatment. b: FR167653 (0.1 μM). c: FR167653 (1 μM). d: FR167653 (10 μM). TRAP-positive MNCs appear as red cells with clear peripheries.
doi:10.1371/journal.pone.0023199.g002

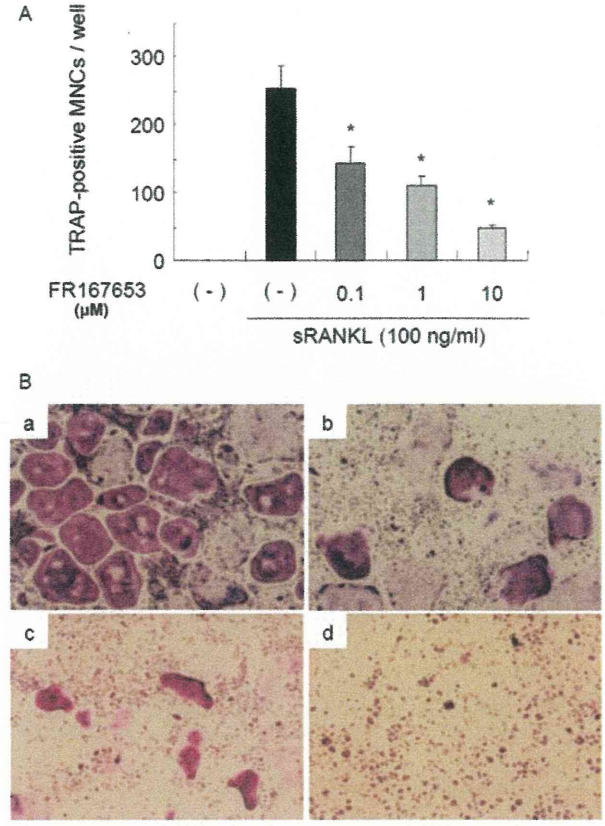

Figure 3. Effects of FR167653 on osteoclast formation in M-CSF-dependent bone marrow macrophages treated with sRANKL. A. Osteoclast formation assay using M-CSF-dependent bone marrow macrophages (MDBMMs) prepared as described in the Materials and Methods section. TRAP-positive MNCs with three or more nuclei were counted as osteoclasts. n = 6. *: $p<0.001$ versus the group treated only with sRANKL. B. TRAP staining for MDBMMs stimulated by sRANKL (100 ng/ml). a: No treatment. b: FR167653 (0.1 μM). c: FR167653 (1 μM). d: FR167653 (10 μM).
doi:10.1371/journal.pone.0023199.g003

Bone marrow stromal cells were obtained by culturing primary bone marrow cells for ten days. Almost all non-adherent or loosely attached hematopoietic cells in the primary bone marrow cell cultures were removed by pipetting each time when the medium was changed. Expression of RANKL and OPG mRNA in bone marrow stromal cells was increased or decreased, respectively, within three days of PTHrP treatment. The increased expression even lasted 6 days post-treatment. Even at a dose of 10 μM, FR167653 has no detectable effect on the PTHrP-mediated expression of RANKL and OPG mRNA (Figure 4). Taken together, these results further suggest that FR167653 acts directly on osteoclast precursors (rather than on stromal cells or osteoblasts) in its role as an inhibitor of osteoclast formation.

Expression of c-Fos and NFATc1 in osteoclast precursors (MDBMMs) were inhibited by FR167653

In order to investigate the mechanism of FR167653 on osteoclast formation in osteocalst precursor cells, we detected the expression of c-Fos and NFATc1 in bone marrow macrophage cells by western blotting and RT-PCR following the FR167653 treatments. As shown in Figure 5, the mRNA expression levels of c-fos and NFATc1 were dramatically increased when treated with sRANKL and these effects were inhibited by FR167653 in a dose-dependent manner($p<0.05$; Figure 5A). Similarly, c-Fos and NFATc1 protein levels were decreased in the presence of FR167653 dose-dependently (Figure 5B).

FR167653 reduces PTHrP-induced bone resorption in vivo

We next examined the effects of FR167653 on PTHrP-induced bone resorption *in vivo*. Animal models of bone resorption were established by direct injection of PTHrP onto the dorsal surface of mice calvaria. Radiographic evidence of bone resorption comprises zones of increased radiolucency in the calvaria. Histologically, these changes are associated with significant periosteal bone resorption on the dorsal calvarial surface and increased marrow spaces, accompanied with increased numbers of osteoclasts. FR167653 significantly reduced the radiographic bone resorption areas ($p<0.05$; Figure 6) and osteoclast number (as determined on histological sections) ($p<0.005$, Figure 7).

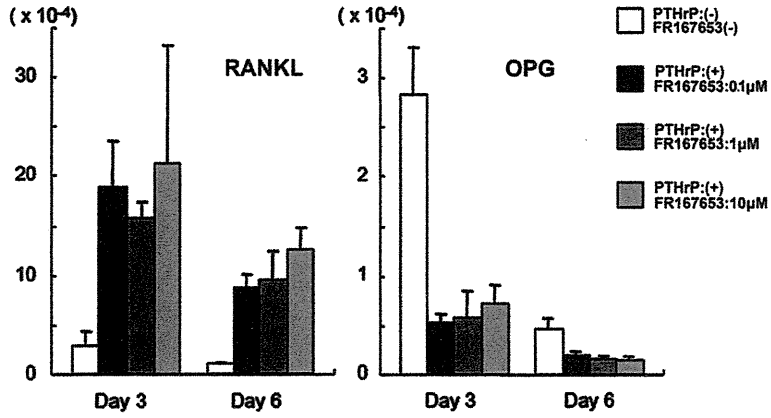

Figure 4. FR167653 does not affect OPG or RANKL expression by PTHrP-treated stromal cells. Bone marrow stromal cells were seeded into six-well plates and treated with PTHrP (90 ng/ml) and FR167653 at various concentrations for three and six days. Real-time PCR was used to determine the OPG or RANKL gene expression levels. The results are shown as mean ±S.D. of three independent experiments. Expression of RANKL and OPG mRNA was increased or decreased, respectively, within three days of PTHrP treatment, and lasted 6 days post-treatment. The expression level of RANKL and OPG did not changed by adding 1 μM or 10 μM FR167653 ($P>0.05$).
doi:10.1371/journal.pone.0023199.g004

Treatment with FR167653 has the effect on the cotnrol of PTHrP-induced systemic hypercalcemia

PTHrP is one of the causative factors of the hypercalcemia that is associated with malignancy, since PTHrP can induce systemic bone resorption. Furthermore, extensive local bone resorption is to some extent a contributory cause of hypercalcemia. For this reason, we monitored whole-blood ionized calcium levels in our experimental system. The level of whole-blood ionized calcium was increased at three hours after PTHrP injection on days 3 and 5 compared to day 1. When additionally treated with FR167653, the whole-blood ionized calcium concentration was significantly decreased at day 3, but not day 5. This suggest the functional involvement of p38 MAPK in PTHrP-induced systemic hypercalcemia (Figure 8).

Discussion

There are several reports about p38 MAPK inhibitor, SB203580, inhibits osteoclast differentiation in RAW264 induced by RANKL [28] or in bone marrow cells induced by 1α, 25-$(OH)_2$ D_3 and prostaglandin E_2 (PGE_2) [14]. Previously, we reported that M-CSF-dependent sRANKL- and TNFα-induced osteoclast formation in primary bone marrow cells, and collagen-induced arthritis in rats were inhibited by FR167653 [23]. Here we further show that FR167653, a selective inhibitor of p38 MAPK, strongly inhibits osteoclast differentiation in PTHrP-treated bone marrow cell cultures.

We also investigated the mechanism of FR167653 involved in the inhibition of osteoclast formation. Most osteoclastgenesis inducers are thought to stimulate osteoclast formation via up-

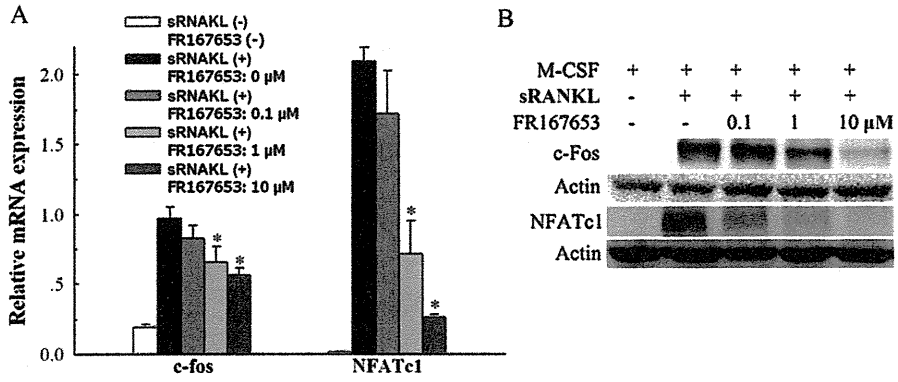

Figure 5. The effects of FR167653 on sRANKL-induced c-Fos and NFATc1 expression level in M-CSF-dependent bone marrow macrophages (MDBMMs). Bone marrow macrophages were treated with 100 ng/ml M-CSF and 100 ng/ml sRANKL without or with FR67653 at the indicated concentration. After 24 h incubation, cells were harvested and subjected to RT-PCR (A). For western blot analysis (B), the cells were incubated for 48 h. Expression of c-Fos and NFATc1 in both mRNA and protein levels were increased following the sRANKL treatment. This enhancement was inhibited by FR167653 in a dose dependent manner. The results are shown as mean ±S.D. of three independent experiments. *: $p<0.05$ versus the group treated only with sRANKL.
doi:10.1371/journal.pone.0023199.g005

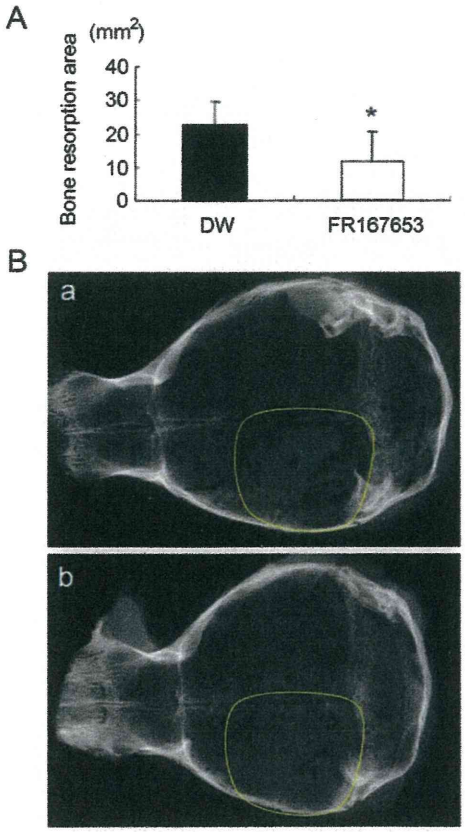

Figure 6. The effect of FR167653 on PTHrP-induced bone resorption. The calvarial bone resorption was measured radiographically on the left side (area marked by yellow line) where treated by direct subcutaneous injection of PTHrP. A. Treatment by FR167653 reduced the bone resorption area (*: P<0.005). DW:distilled water. B. Representative X-rays of mouse calvaria with PTHrP-induced bone resorption. a: control group (treated with DW). b: FR167653 treatment group.
doi:10.1371/journal.pone.0023199.g006

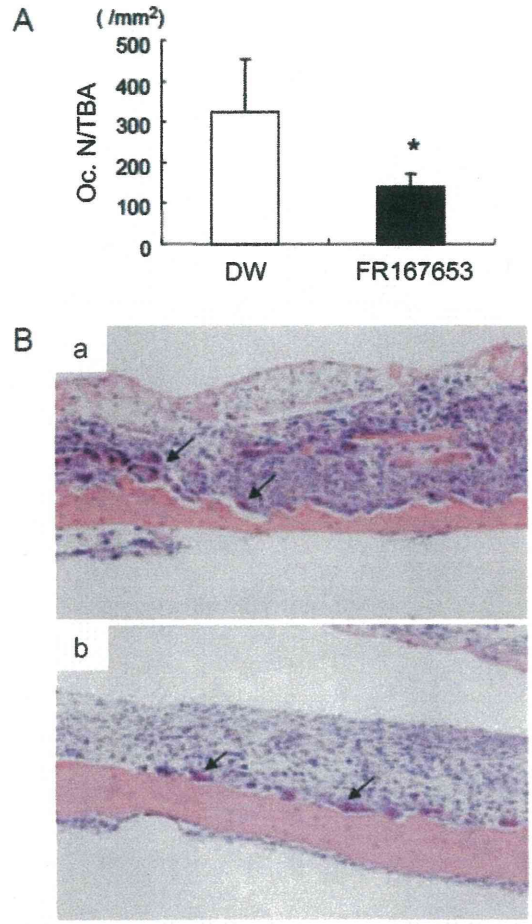

Figure 7. The effects of FR167653 on osteoclast number in calvaria from PTHrP-treated animals. A. Osteoclast number per unit bone area (OcN-BTA) was measured histologically as described in the Materials and Methods section. Treatment of FR167653 reduces the number of osteoclasts (*: P<0.005). B. TRAP staining and counterstain with hematoxylin on calvaria sections. a: Histological section of animals treated with DW. b: Histological section of animals treated with FR167653. Osteoclasts are indicated by arrowheads.
doi:10.1371/journal.pone.0023199.g007

regulation of RANKL and down-regulation of OPG gene expression as mediated by osteoblast or bone marrow stromal cells [25,29]. In our study, however, even the highest concentration of FR167653 that was tested (10 μM) has no effect on RANKL and OPG expression by PTHrP-stimulated primary bone marrow stromal cells. These data suggest that p38 MAPK is not involved in the regulation of PTHrP-mediated bone resorption-related functions of osteoblasts, including regulation of RANKL and OPG expression. This is consistent with previous results that SB203580 has no effect on RANKL and OPG expression by primary osteoblast stimulated with 1α, 25- $(OH)_2D_3$ and PGE_2 [14]. Together, the data suggest that p38 MAPK is involved in the differentiation of osteoclast precursors, rather than in the function of supporting cell such as osteoblasts or bone marrow stromal cells.

However, the current study found that the up-regulation of c-Fos and NFATc1expression treated with RANKL in osteoclast precursor cells (MDBMMs) were inhibited by FR167653 in a dose-dependent manner in both mRNA and protein levels. This strongly suggested the inhibition of osteoclast differentiation by FR167653 is involved in regulating c-Fos and NFATc1 expression in osteoclast precursor cells. The similar results were reported by using SB203580 [30]. These findings, together with the present study, suggest that p38 MAPK-mediated signal propagation down to c-Fos and NFATc1 are of fundamental importance for the differentiation of osteoclast precursors into osteoclasts.

In our animal experiments, local injection of PTHrP on calvaria caused significant bone resorption and systemic hypercalcemia, and increased osteoclast number. Treatment with FR167653 successfully reduced bone resorption and osteoclast number in calvaria, and eventually protected the calvaria from serious osteoclastic dystruction induced by locally administered PTHrP. However, some relieving effect on hypercalcemia was observed. In our hands, inhibition of p38 MAPK by FR167653 significantly decreased the whole-blood calcium level on day 3. However, there is no difference in blood calcium level between the FR167653 treatment group and the control group at day 5.

It was reported that recombinant human OPG is effective in inhibiting bone resorption and hypercalcemia induced by PTHrP *in vivo* [27]. Treatment with chimeric form of OPG in combination with PTHrP (20 μg/day) maintained whole blood ionized calcium

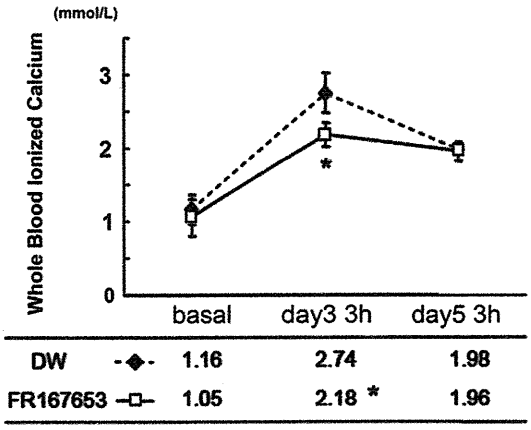

Figure 8. The effect of FR167653 on whole-blood ionized calcium levels in PTHrP-treated mice. PTHrP induces a significant elevation of whole-blood ionized calcium levels in mice within three hours of injection with PTHrP (at day three and five). The whole-blood ionized calcium levels are lower in the FR167653-treated group than in the DW-treated group (control group) at day three (*: $P<0.05$). By day five, however, there was no significant difference between two groups.
doi:10.1371/journal.pone.0023199.g008

levels within the normal range (~1.20 mmol/l). Even though FR167653 was given subcutaneously, it should have act systemically. The concentration of calcium in extracellular fluids is under control by a complex homeostatic system strictly that includes the parathyroid glands, kidneys, bones, and intestines [31,32]. An increase of extracellular calcium concentration is sensed by a calcium-sensing receptor (CaR) in the plasma membrane of parathyroid gland cells and the kidney which in turn affects parathyroid hormone, calcitonin, and 1, 25 $(OH)_2D_3$ secretion. Although intracellular signaling systems regulated by the CaR are still in obscurity, recent evidence suggests that MAPK pathways are activated by CaR [33,34]. For example, calcium homeostasis by angiotensin II in adrenal glomerulosa cells is mediated by activation of p38 MAPK pathways [35]. These observations may help us to understand the surprisingly small effect of p38 MAPK pathway blockade on regulating hypercalcemia induced by PTHrP because the inhibition of p38 MAPK pathway may block CaR signaling pathway as well, which in turn causes reduced reaction to extracellular Ca^{2+} in tissues that express CaR. The detailed mechanism for why inhibition of p38 MAPK partially prevents hypercalcemia even though it is effective in reducing bone resorption merits further studies.

FR167653 has been used in several inflammatory disease models and no obvious adverse events were observed [15–19]. In our previous *in vivo* study [23], we found no significant side effects with daily treatments of 32 mg/kg, a dose found to be safe and effective in other inflammation models as well [36]. In the present study, we also found that there is no significant side effects when twice daily treatment with 30 mg/kg FR167653 for about 1 week. Long-term injection of FR167653 may lead to toxic events; indeed, one study demonstrated that FR167653 treatment increased plasma creatine and lactate dehydrogenase levels in rats [37]. Clearly, the potentially adverse effects of FR167653, including its modulation of calcium homeostasis, need to be studied extensively.

In conclusion, our data indicate that a potent p38 MAPK inhibitor, FR167653, blocks PTHrP-induced osteoclastogenesis *in vitro*, and bone resorption and hypercalcemia *in vivo*. Our results indicate that the responses of other tissues or organs to the p38 MAPK inhibitor may affect calcium homeostasis. This study provides a plausible explanation and target for PTHrP-induced osteoclastogenesis, which will help us to understand the mechanism of bone resorption-related diseases.

Acknowledgments

We thank Dr. Noriyuki Tsumaki for his helpful discussion. We also thank Miss Kanae Asai and Miss Mizuki Nakata for their excellent technical assistance.

Author Contributions

Conceived and designed the experiments: AM. Performed the experiments: HT. Analyzed the data: HT. Contributed reagents/materials/analysis tools: MO. Wrote the paper: MN.

Reference

1. Wysolmerski JJ, Broadus AE (1994) Hypercalcemia of malignancy: the central role of parathyroid hormone-related protein. Annu Rev Med 45: 189–200.
2. Guise TA, Yin JJ, Taylor SD, Kumagai Y, Dallas M, et al. (1996) Evidence for a causal role of parathyroid hormone-related protein in the pathogenesis of human breast cancer-mediated osteolysis. J Clin Invest 98: 1544–1549.
3. Yin JJ, Selander K, Chirgwin JM, Dallas M, Grubbs BG, et al. (1999) TGF-beta signaling blockade inhibits PTHrP secretion by breast cancer cells and bone metastases development. J Clin Invest 103: 197–206.
4. Mundy GR, Yoneda T (1998) Bisphosphonates as anticancer drugs. N Engl J Med 339: 398–400.
5. Coleman RE, Lipton A, Roodman GD, Guise TA, Boyce BF, et al. (2010) Metastasis and bone loss: advancing treatment and prevention. Cancer Treat Rev 36: 615–620.
6. Thomas RJ, Guise TA, Yin JJ, Elliott J, Horwood NJ, et al. (1999) Breast cancer cells interact with osteoblasts to support osteoclast formation. Endocrinology 140: 4451–4458.
7. Lacey DL, Timms E, Tan HL, Kelley MJ, Dunstan CR, et al. (1998) Osteoprotegerin ligand is a cytokine that regulates osteoclast differentiation and activation. Cell 93: 165–176.
8. Yasuda H, Shima N, Nakagawa N, Yamaguchi K, Kinosaki M, et al. (1998) Osteoclast differentiation factor is a ligand for osteoprotegerin/osteoclastogenesis-inhibitory factor and is identical to TRANCE/RANKL. Proc Natl Acad Sci U S A 95: 3597–3602.
9. Kong YY, Yoshida H, Sarosi I, Tan HL, Timms E, et al. (1999) OPGL is a key regulator of osteoclastogenesis, lymphocyte development and lymph-node organogenesis. Nature 397: 315–323.
10. Jimi E, Furuta H, Matsuo K, Tominaga K, Takahashi T, et al. (2011) The cellular and molecular mechanisms of bone invasion by oral squamous cell carcinoma. Oral Dis 17: 462–468.
11. Bucay N, Sarosi I, Dunstan CR, Morony S, Tarpley J, et al. (1998) osteoprotegerin-deficient mice develop early onset osteoporosis and arterial calcification. Genes Dev 12: 1260–1268.
12. Anandarajah AP (2009) Role of RANKL in bone diseases. Trends Endocrinol Metab 20: 88–94.
13. Matsumoto M, Sudo T, Saito T, Osada H, Tsujimoto M (2000) Involvement of p38 mitogen-activated protein kinase signaling pathway in osteoclastogenesis mediated by receptor activator of NF-kappa B ligand (RANKL). J Biol Chem 275: 31155–31161.
14. Li X, Udagawa N, Itoh K, Suda K, Murase Y, et al. (2002) p38 MAPK-mediated signals are required for inducing osteoclast differentiation but not for osteoclast function. Endocrinology 143: 3105–3113.
15. Yamamoto N, Sakai F, Yamazaki H, Nakahara K, Okuhara M (1996) Effect of FR167653, a cytokine suppressive agent, on endotoxin-induced disseminated intravascular coagulation. Eur J Pharmacol 314: 137–142.
16. Yamamoto N, Sakai F, Yamazaki H, Sato N, Nakahara K, et al. (1997) FR167653, a dual inhibitor of interleukin-1 and tumor necrosis factor-alpha, ameliorates endotoxin-induced shock. Eur J Pharmacol 327: 169–174.
17. Takahashi S, Keto Y, Fujita T, Uchiyama T, Yamamoto A (2001) FR167653, a p38 mitogen-activated protein kinase inhibitor, prevents Helicobacter pylori-induced gastritis in Mongolian gerbils. J Pharmacol Exp Ther 296: 48–56.
18. Cau J, Favreau F, Zhang K, Febrer G, de la Motte GR, et al. (2009) FR167653 improves renal recovery and decreases inflammation and fibrosis after renal ischemia reperfusion injury. J Vasc Surg 49: 728–740.
19. Yoshinari D, Takeyoshi I, Koibuchi Y, Matsumoto K, Kawashima Y, et al. (2001) Effects of a dual inhibitor of tumor necrosis factor-alpha and interleukin-1 on lipopolysaccharide-induced lung injury in rats: involvement of the p38 mitogen-activated protein kinase pathway. Crit Care Med 29: 628–634.

20. Nishikori T, Irie K, Suganuma T, Ozaki M, Yoshioka T (2002) Anti-inflammatory potency of FR167653, a p38 mitogen-activated protein kinase inhibitor, in mouse models of acute inflammation. Eur J Pharmacol 451: 327–333.
21. Furuichi K, Wada T, Iwata Y, Sakai N, Yoshimoto K, et al. (2002) Administration of FR167653, a new anti-inflammatory compound, prevents renal ischaemia/reperfusion injury in mice. Nephrol Dial Transplant 17: 399–407.
22. Hou Z, Yanaga K, Kamohara Y, Eguchi S, Tsutsumi R, et al. (2003) A new suppressive agent against interleukin-1beta and tumor necrosis factor-alpha enhances liver regeneration after partial hepatectomy in rats. Hepatol Res 26: 40–46.
23. Nishikawa M, Myoui A, Tomita T, Takahi K, Nampei A, et al. (2003) Prevention of the onset and progression of collagen-induced arthritis in rats by the potent p38 mitogen-activated protein kinase inhibitor FR167653. Arthritis Rheum 48: 2670–2681.
24. Azuma Y, Kaji K, Katogi R, Takeshita S, Kudo A (2000) Tumor necrosis factor-alpha induces differentiation of and bone resorption by osteoclasts. J Biol Chem 275: 4858–4864.
25. Huang H, Chang EJ, Ryu J, Lee ZH, Lee Y, et al. (2006) Induction of c-Fos and NFATc1 during RANKL-stimulated osteoclast differentiation is mediated by the p38 signaling pathway. Biochem Biophys Res Commun 351: 99–105.
26. Boyce BF, Aufdemorte TB, Garrett IR, Yates AJ, Mundy GR (1989) Effects of interleukin-1 on bone turnover in normal mice. Endocrinology 125: 1142–1150.
27. Morony S, Capparelli C, Lee R, Shimamoto G, Boone T, et al. (1999) A chimeric form of osteoprotegerin inhibits hypercalcemia and bone resorption induced by IL-1beta, TNF-alpha, PTH, PTHrP, and 1, 25(OH)2D3. J Bone Miner Res 14: 1478–1485.
28. Matsumoto M, Sudo T, Maruyama M, Osada H, Tsujimoto M (2000) Activation of p38 mitogen-activated protein kinase is crucial in osteoclastogenesis induced by tumor necrosis factor. FEBS Lett 486: 23–28.
29. Brandstrom H, Jonsson KB, Ohlsson C, Vidal O, Ljunghall S, et al. (1998) Regulation of osteoprotegerin mRNA levels by prostaglandin E2 in human bone marrow stroma cells. Biochem Biophys Res Commun 247: 338–341.
30. Horwood NJ, Elliott J, Martin TJ, Gillespie MT (1998) Osteotropic agents regulate the expression of osteoclast differentiation factor and osteoprotegerin in osteoblastic stromal cells. Endocrinology 139: 4743–4746.
31. Magno AL, Ward BK, Ratajczak T (2011) The calcium-sensing receptor: a molecular perspective. Endocr Rev 32: 3–30.
32. Brown EM, MacLeod RJ (2001) Extracellular calcium sensing and extracellular calcium signaling. Physiol Rev 81: 239–297.
33. Tfelt-Hansen J, MacLeod RJ, Chattopadhyay N, Yano S, Quinn S, et al. (2003) Calcium-sensing receptor stimulates PTHrP release by pathways dependent on PKC, p38 MAPK, JNK, and ERK1/2 in H-500 cells. Am J Physiol Endocrinol Metab 285: E329–337.
34. Morgan R, Fairfax B, Pandha HS (2006) Calcium insensitivity of FA-6, a cell line derived from a pancreatic cancer associated with humoral hypercalcemia, is mediated by the significantly reduced expression of the Calcium Sensitive Receptor transduction component p38 MAPK. Mol Cancer 5: 51.
35. Startchik I, Morabito D, Lang U, Rossier MF (2002) Control of calcium homeostasis by angiotensin II in adrenal glomerulosa cells through activation of p38 MAPK. J Biol Chem 277: 24265–24273.
36. Wada T, Furuichi K, Sakai N, Iwata Y, Yoshimoto K, et al. (2000) A new anti-inflammatory compound, FR167653, ameliorates crescentic glomerulonephritis in Wistar-Kyoto rats. J Am Soc Nephrol 11: 1534–1541.
37. Gardiner SM, Kemp PA, March JE, Bennett T (1999) Influence of FR167653, an inhibitor of TNF-alpha and IL-1, on the cardiovascular responses to chronic infusion of lipopolysaccharide in conscious rats. J Cardiovasc Pharmacol 34: 64–69.

Biochemical and Biophysical Research Communications 411 (2011) 774–779

Contents lists available at ScienceDirect

Biochemical and Biophysical Research Communications

journal homepage: www.elsevier.com/locate/ybbrc

Spleen tyrosine kinase suppresses osteoblastic differentiation through MAPK and PKCα

Kiyoshi Yoshida, Chikahisa Higuchi *, Akio Nakura, Hideki Yoshikawa

Department of Orthopaedic Surgery, Graduate School of Medicine, Osaka University, Suita, Osaka, Japan

ARTICLE INFO

Article history:
Received 5 July 2011
Available online 18 July 2011

Keywords:
Spleen tyrosine kinase (Syk)
MC3T3-E1 cells
Osteoblastic differentiation
MAPK
PKCα

ABSTRACT

Spleen tyrosine kinase (Syk) is a non-receptor protein kinase present in abundance in a wide range of hematopoietic cells. Syk reportedly plays a crucial role in immune signaling in B cells and cells bearing Fcγ-activation receptors. The role of syk in osteoblastic differentiation has not been well elucidated. We report herein the role of syk in osteoblastic differentiation. We investigated the effects of two syk inhibitors on osteoblastic differentiation in mouse preosteoblastic MC3T3-E1 cells and bone marrow stromal ST2 cells. Expression of syk was detected in these two cell lines. Two syk inhibitors stimulated mRNA expression of osteoblastic markers (ALP, Runx2, Osterix). Mineralization of extracellular matrix was also promoted by treatment with syk inhibitors. Knockdown of Syk caused increased mRNA expression of osteoblastic markers. In addition, syk inhibitor and knockdown of Syk suppressed phosphorylation of mitogen-activated protein kinase (MAPK) and protein kinase Cα (PKCα). Our results indicate that syk might regulate osteoblastic differentiation through MAPK and PKCα.

1. Introduction

Spleen tyrosine kinase (Syk) is a non-receptor protein kinase present in abundance in various hematopoietic cells, including mast cells, neutrophils, macrophages, natural killer cells, and dendritic cells [1–6]. Syk contains 2 Src homology (SH2) domains in tandem and multiple autophosphorylation sites, and is activated upon binding of the tandem SH2 domains to an immunoreceptor tyrosine-based activating motif (ITAM). Syk translocates to the phosphorylated ITAM motifs via the interaction of the SH2 domains and undergoes conformational changes upon autophosphorylation and binding to phosphorylated ITAM. Subsequently, Syk to ITAM motifs leads to phosphorylation of a number of molecules [7–9]. As a consequence, activation of Syk promotes the downstream functional responses following immunoreceptor activation, proliferation, differentiation and effector functions such as degranulation, respiratory burst and cytokine release.

The importance of the roles of Syk in immunoreceptor-mediated signaling pathways and biological functions has been established [10–12]. In the field of bone metabolism, the roles of Syk in osteoclast differentiation and osteoclast function have been intensively studied. Osteoclasts are macrophage-related bone-resorbing cells that develop from early myeloid precursors under the control of the receptor activator of nuclear factor-κB (RANK) ligand expressed by osteoblasts. Loss-of-function mutations of DAP12 cause bone abnormalities in humans, indicating a role of ITAM-based signaling in bone metabolism [13]. DAP12-deficient mice show moderate osteopetrosis [14,15], whereas mice lacking both DAP12 and FcRγ show severe osteopetrosis [16,17]. Syk is activated downstream of DAP12 and FcRγ in an ITAM-dependent manner and is also required for osteoclast development and function [18,19].

Osteoblastic differentiation is an essential step in bone formation. During the differentiation of mesenchymal cells into osteoblasts, expression of type I collagen (Col I) is one of the earliest events, followed by expression of alkaline phosphatase (ALP). Osteocalcin (OCN) is secreted in the late stage of osteoblastic differentiation, with mineralization of extracellular matrix as the final step. The role of Syk in osteoblastic differentiation has not been well elucidated and no reports has clarified the functions of Syk in osteoblasts. Here, we examined the promotive functions of Syk on osteoblastic differentiation of mesenchymal cell lines.

2. Materials and methods

2.1. Cell culture

Mouse preosteoblastic MC3T3-E1 cells and bone marrow stromal ST2 cells were obtained from Riken Cell Bank (Tsukuba, Japan). MC3T3-E1 cells were cultured in α-minimal essential medium (α-MEM; Invitrogen, Carlsbad, CA, USA) supplemented with 10% fetal

* Corresponding author. Address: Department of Orthopaedic Surgery, Graduate School of Medicine, Osaka University, 2-2 Yamadaoka, Suita, Osaka 565-0871, Japan. Fax: +81 6 6879 3559.
E-mail address: c-higuchi@umin.ac.jp (C. Higuchi).

0006-291X/$ - see front matter © 2011 Elsevier Inc. All rights reserved.
doi:10.1016/j.bbrc.2011.07.023

bovine serum (FBS) (Hyclone, Road Logan, UT, USA) (growth medium) at 37 °C under a humidified atmosphere of 5% CO_2. ST2 cells were cultured in RPMI 1640 (Invitrogen) containing 10% FBS. For each assay, the growth medium was replaced with growth medium supplemented with 0.2 mM ascorbic acid (Sigma–Aldrich, St. Louis, MO, USA) and 4 mM β-glycerophosphate (Sigma–Aldrich) (differentiation medium). The medium was changed twice per week.

2.2. Proliferation assay

MC3T3-E1 cells were cultured in 48-well plates at a concentration of 2.0×10^4 cells/cm^2 in differentiation medium. Cell proliferation was assessed using the Premix WST-1 cell proliferation assay system (Takara Bio, Otsu, Japan) according to the instructions from the manufacturer. This assay was performed every 24 h.

2.3. Alkaline phosphatase (ALP) staining

MC3T3-E1 cells were seeded in a 24-well plate at a density of 2.0×10^4 cells/cm^2. After 24 h of incubation, cells were treated with a Syk inhibitor II, Syk inhibitor IV (Calbiochem, San Diego, Ca, USA) in differentiation medium for 3 days. For ALP staining, cells were washed with phosphate-buffered saline (PBS) (Sigma–Aldrich) and fixed for 15 min with 10% formalin at room temperature. After fixation, cells were incubated with the ProtoBlot® II AP System with Stabilized Substrate (Promega, Madison, WI, USA) for 1 h at room temperature.

2.4. Alizarin Red S staining

MC3T3-E1 cells were cultured for 28 days on BIOCOAT® 24-well plates (Nippon Becton Dickinson, Tokyo, Japan) in differentiation medium. The cells were then washed twice with PBS, fixed in 10% formalin for 10 min and then stained with Alizarin Red S (Sigma–Aldrich) at pH 6.3 for 1 h. After discarding the Alizarin Red S solution and washing the cells three times with distilled water, bound Alizarin Red was dissolved in 200 μL of 100 mM hexadecylpyridium chloride (Sigma–Aldrich) and absorbance of the supernatant was measured at 570 nm.

2.5. Reverse transcription PCR (RT-PCR) and quantitative real-time PCR

Total RNA was isolated from cells using TRIzol (Invitrogen) according to the instructions from the manufacturer. Synthesis of cDNA was achieved using a Transcriptor First Strand cDNA Synthesis kit (Roche Diagnostics, Mannheim, Germany).

RT-PCR was performed using PCR Master Mix (Promega) and appropriate primer pairs. Sequences of the specific primers used for RT-PCR are shown in Table 1. PCR products were separated by agarose gel electrophoresis and detected with ethidium bromide.

Each mRNA was measured using a quantitative real-time PCR assay, employing LightCycler® TaqMan® Master (Roche Diagnostics), a Universal ProbeLibrary Probe (UPL Probe; Roche Diagnostics), and an appropriate pair of primers according to the protocol described by the manufacturer. Sequences of the specific primers and UPL Probes used are shown in Table 2. Expression values were normalized to GAPDH.

2.6. Western blotting

Cells were rapidly lysed on ice using Blue Loading Buffer Reagents (Cell Signaling Technology, Beverly, MA, USA) containing 0.125 M dithiothreitol. These samples were subjected to 8% SDS–PAGE, then transferred onto nitrocellulose membranes (Bio-Rad Laboratories, Hercules, CA, USA). After blocking with 0.1% Tween20-added PBS (T-PBS) containing 3% bovine serum albumin (Sigma–Aldrich), membranes were incubated with specific primary antibodies against Syk (Santa Cruz Biotechnology, Austin, TX, USA), p42/44 MAPK, phosphor-p42/44 MAPK (Thr202/Tyr204), PKCα, phosho-PKC (pan) (βII Ser660), phosho-PKCα/βII (Thr638/641) (Cell Signaling Technology), and β-actin (Sigma–Aldrich). Secondary anti-immunoglobulin G antibodies (alkaline phosphatase-conjugated anti-mouse or anti-rabbit) were incubated for 1 h at room temperature in 0.1% T-PBS. Immunoreactive bands were visualized using the ProtoBlot® II AP System and Stabilized Substrate (Promega).

2.7. Knockdown of Syk using RNA interference

MC3T3-E1 cells were transfected with small interfering RNA (siRNA) using Lipofectamine RNAiMAX (Invitrogen) according to the reverse transfection method in the manufacturer's protocol. Two different sets of Syk siRNA oligos were used for knockdown of Syk, as follows: site 1 (5′-GGGAAGAGGCUGAAGACUA-3′ and 5′-UAGUCUUCAGCCUCUUCCCTT-3′); site 2 (5′-GGACUUACGAUGUGGAGAATT-3′ and 5′-UUCUCCACAUCGUAAGUCCTT-3′) (B-Bridge International, Inc., Sunnyvale, CA, USA). Control siRNA was purchased from B-Bridge International, Inc. MC3T3-E1 cells transfected with siRNA were seeded in 24-well plates at a concentration of 1.0×10^4 cells/cm^2 for 48 h. The medium was then replaced with differentiation medium and the cells were incubated for 3 days prior to use for experiments.

2.8. Statistical analysis

All data are expressed as means ± standard deviation (SD) and a minimum of three independent experiments were performed for each assay. Statistical analysis was performed using a two-sided unpaired Student's *t*-test, or analysis of variance (ANOVA) for multiple comparisons. Differences between experimental groups were considered significant for values of $p < 0.05$.

Table 1
Sequences of PCR primers used to amplify each of genes in RT-PCR.

Gene	Primer	Sequence (5′–3′)
ALP	Forward	GCCCTCTCCAAGACATATA
	Reverse	CCATGATCACGTCGATATCC
Osteocalcin	Forward	CAAGTCCCACACAGCAGCTT
	Reverse	AAAGCCGAGCTGCCAGAGTT
Runx2	Forward	GCTTGATGACTCTAAACCTA
	Reverse	AAAAAGGGCCCAGTTCTGAA
Osterix	Forward	GAAGAAGCTCACTATGGCTC
	Reverse	GAAAAGCCAGTTGCAGACGA
GAPDH	Forward	TGAACGGGAAGCTCACTGG
	Reverse	TCCACCACCCTGTTGCTGTA

Table 2
Sequences of PCR primers and specific probes used for quantitative real-time PCR.

Gene	UPL probe no.	Primer	Sequence (5′–3′)
ALP	81	Forward	ACTCAGGGCAATGAGGTCAC
		Reverse	CACCCGAGTGGTAGTCACAA
Osteocalcin	71	Forward	CACCATGAGGACCCTCTCTC
		Reverse	TGGACATGAAGGCTTTGTCA
Runx2	34	Forward	GCCCAGGCGTATTTCAGAT
		Reverse	TGCCTGGCTCTTCTTACTGAG
Osterix	106	Forward	CTCCTGCAGGCAGTCCTC
		Reverse	GGGAAGGGTGGGTAGTCATT
GADPH	80	Forward	TGTCCGTCGTGGATCTGAC
		Reverse	CCTGCTTCACCACCTTCTTG

3. Results

3.1. Osteoblastic differentiation of MC3T3-E1 cells is promoted by Syk inhibitors

Prior to determination of the functions of Syk on osteoblastic differentiation, we first evaluated the endogenous expression of Syk in MC3T3-E1 cells by Western blotting. Expression of Syk was identified in MC3T3-E1 cells (Fig. 1A). To investigate the function of Syk in osteoblastic cells, we examined effects of a syk inhibitor, Syk inhibitor II, on osteoblastic differentiation. We first measured the proliferation of MC3T3-E1 cells with various concentration of Syk inhibitor II. Proliferation was decreased with high concentrations of Syk inhibitor II at days 3 and 4 (Fig. 1B). Treatment with the Syk inhibitor II induced strong ALP staining in a dose-dependent manner (Fig. 1C). Furthermore, Alizarin Red S staining indicated that Syk inhibitor II clearly promoted calcification of the extracellular matrix (ECM) in MC3T3-E1 cells (Fig. 1D, upper panel). The degree of ECM calcification was quantified by measuring the absorbance of Alizarin Red S solution (Fig. 1D, lower graph). In addition, quantitative real-time PCR assay showed acceleration of mRNA expression for ALP, one of the early osteoblastic differentiation markers, and of two transcription factors, Runx2 and Osterix following treatment with Syk inhibitor II (Fig. 1D).

To further confirm function of the Syk inhibitor in osteoblastic cells, we examined the effects of another Syk inhibitor, Syk inhibitor IV, on osteoblastic differentiation. Similar to Syk inhibitor II, proliferation decreased with high concentrations of Syk inhibitor IV on days 3 and 4. Treatment with Syk inhibitor IV also induced the promotion of ALP staining and mineralization of ECM in a dose-dependent manner. Moreover, mRNA transcript of two osteoblastic markers (ALP and OCN) and two osteoblastic transcriptional factors (Runx2 and Osterix) were increased by Syk inhibitor IV (Supplementary Fig. S1). These findings indicate that inhibition of Syk promotes osteoblastic differentiation in MC3T3-E1 cells and suggest that Syk might play a suppressive role in osteoblastic differentiation in MC3T3-E1 cells.

3.2. Osteoblastic differentiation of bone marrow stromal ST2 cells is promoted by Syk inhibitor

To further confirm effects of syk inhibition on osteoblastic differentiation, we investigated the effects of Syk inhibitor II on osteoblastic differentiation in bone marrow stromal ST2 cells. First, we identified endogenous expression of syk in ST2 cells by Western blotting (Supplementary Fig. S2A). Quantitative real-time PCR assay showed acceleration of the mRNA expressions of ALP, OCN, and Osterix by Syk inhibitor II in a dose-dependent manner, as

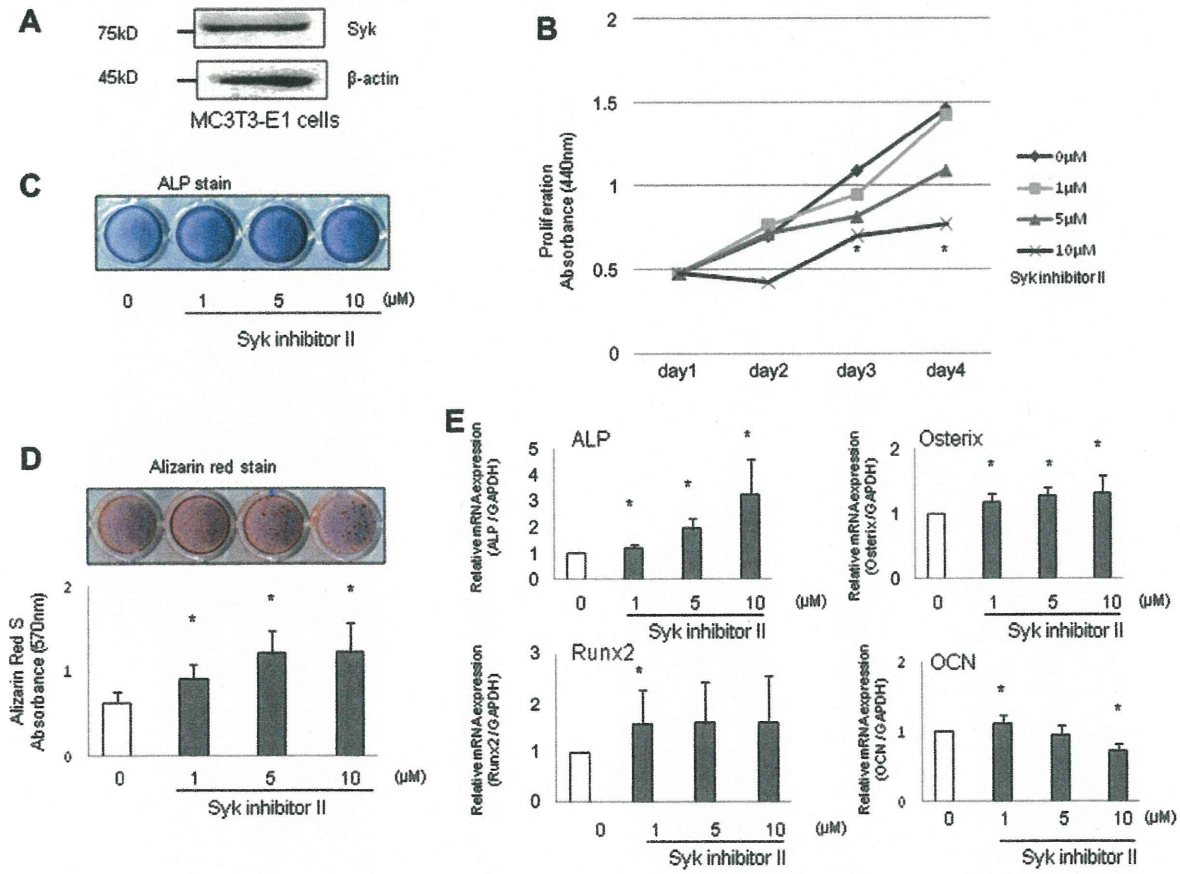

Fig. 1. Osteoblastic differentiation of MC3T3-E1 cells promoted by the Syk inhibitor II. (A) Endogenous expression of the Syk protein in MC3T3-E1 cells by Western blotting. β-Actin was used as the internal control. (B) Proliferation of MC3T3-E1cells with various concentration of Syk inhibitor II. MC3T3-E1 cells were incubated for 1 day following which the medium was treated with various concentration of Syk inhibitor II for 3 days. Cell proliferation was assayed at daily intervals over these 4 days of incubation. (C) ALP staining and activity of MC3T3-E1 cells treated with Syk inhibitor II. MC3T3-E1 cells (2.0×10^4 cells/cm^2) were cultured in growth medium for 24 h, and then replaced with the Syk inhibitor II in differentiation medium for 3 days. (D) MC3T3-E1 cells stained with Alizarin Red solution and quantified Ca content in the matrix of the cells. MC3T3-E1 cells were cultured with the Syk inhibitor II in differentiation medium for 28 days. Fresh medium was changed twice per week. (E) Total RNA isolated from MC3T3-E1 cells treated with the Syk inhibitor II for 3 days. mRNA expression of the osteoblast-related genes: ALP, OCN; the transcription factor Runx2, and the gene Osterix was determined using quantitative real-time PCR analysis and UPL probes. The expression of each gene was normalized to GAPDH expression. (B,C, D and E) Data are means ± SD of three independent experiments performed in duplicate (*: $p < 0.05$ compared with the Syk inhibitor II-untreated control).

for MC3T3-E1 cells (Supplementary Fig. S2B). Expression of Runx2 tended to increase in a dose-dependent manner. These results showed Syk might have a suppressive effect on osteoblastic differentiation in bone marrow stromal ST2 cells.

3.3. Knockdown of Syk promotes osteoblastic differentiation

To further confirm functions of Syk in osteoblastic differentiation, we investigated changes in cell differentiation following knockdown of Syk using an RNA interference method. Fig. 2A shows the low cellular expression level of Syk at 48 h after transfection of two different Syk siRNAs. Quantitative real-time PCR analysis revealed that gene expressions of ALP and OCN were increased by knockdown of Syk in a Syk expression-dependent fashion. Furthermore, knockdown of Syk increased mRNA expression of the transcription factor Runx2 (Fig. 2B). Expression of Osterix was increased with siSyk-1, but decreased with siSyk-2. These results indicate that Syk may suppress osteoblastic differentiation via upregulation of Runx2 expression.

3.4. Syk inhibitor and knockdown of Syk suppress MAPK phosphorylation and PKCα phosphorylation

Syk is known to play a critical role in immune receptor-mediated activation of mitogen-activated protein kinase (MAPK) and phospholipase D (PLD). In addition, treatment of many cell types with phorbol esters stimulates PLD activity, implying regulation of the enzyme by protein kinase C (PKC). To elucidate the effects of Syk on osteoblastic differentiation-related signaling, we studied ERK-MAPK and PKC signaling with the Syk inhibitor in MC3T3-E1 cells. First, Syk inhibitors suppressed p42/44 MAPK phosphorylation in a dose-dependent manner (Fig. 3A). Second, Syk inhibitor suppressed PKC phosophorylation (βII Ser660) (Fig. 3B). Our laboratory recently reported that MAPK and PKCα suppress osteoblastic differentiation [20,21]. We therefore investigated phosphorylation of PKCα. The Syk inhibitor suppressed PKCα/βII (Thr638/641) phosphorylation in a dose-dependent manner. In our previous report, PKCα expressed in MC3T3-E1 cells, but PKCβII was not expressed [21]. These results suggest that Syk inhibition might cause inactivation of MAPK and PKCα. And we studied ERK-MAPK and PKC signaling with knockdown of Syk using a RNA interference in MC3T3-E1 cells. Knockdown of Syk also suppressed p42/44 MAPK phosphorylation and PKCα/βII (Thr638/641) phosphorylation (Fig. 3C, D).

4. Discussion

Syk has been reported to play critical roles in immunoreceptor-related signaling and immune functions such as B- and T-cell development. Syk is also known to be involved in the maintenance of vascular integrity, and proper partitioning of the vascular and

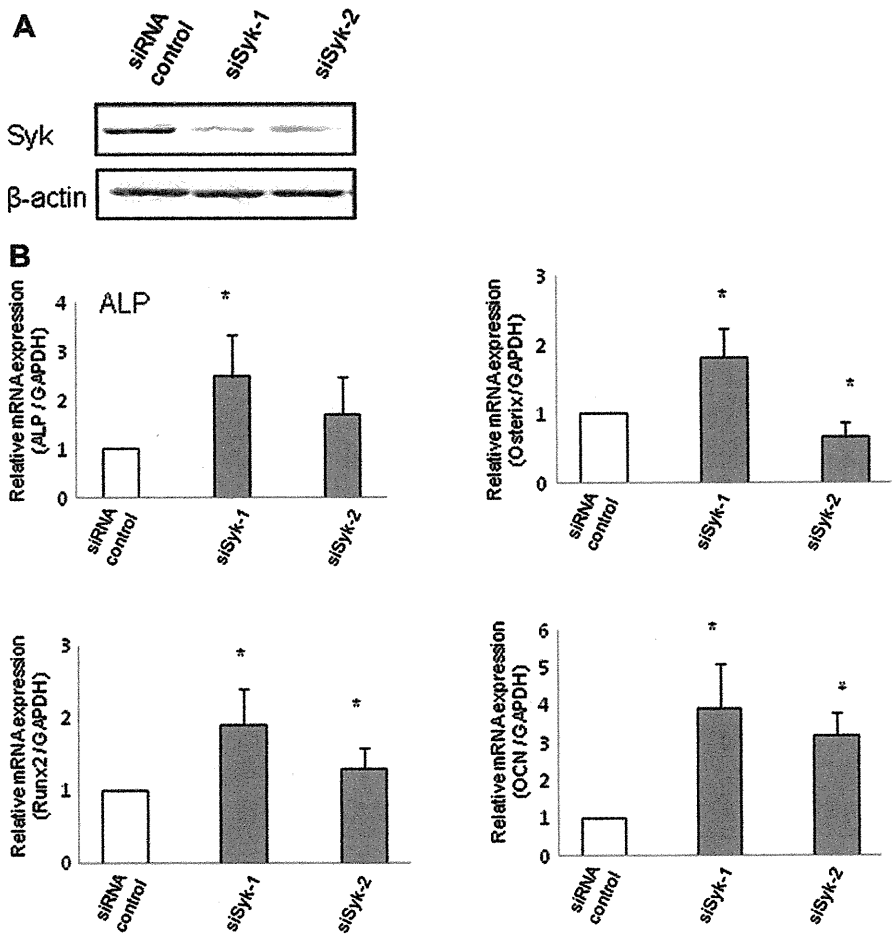

Fig. 2. Knockdown of Syk stimulates osteoblastic differentiation. (A) Western blotting analysis of Syk knockdown in MC3T3-E1 cells by transfection with control or Syk (sites 1 and 2) siRNA. The cells transfected with siRNA were cultured for 48 h. Western blotting was performed using cell lysates as described in Section 2. (B) Expression of osteoblastic-related genes in MC3T3-E1 cells transfected with control and Syk siRNA was assessed by quantitative real-time PCR. Total RNA was extracted from MC3T3-E1 cells. The expression of each gene was normalized against GAPDH expression. Data are means ± SD of three independent experiments performed in duplicate (*: $p < 0.05$ compared with siRNA control).

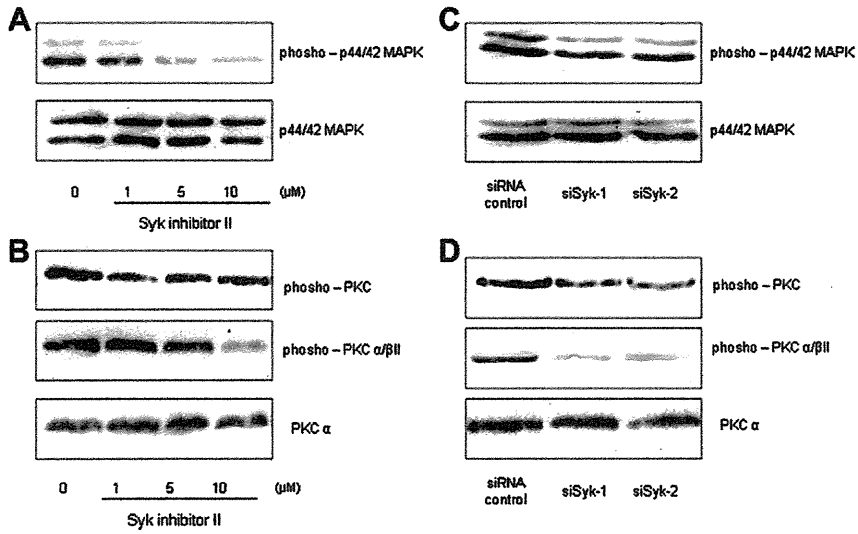

Fig. 3. Effects of the Syk inhibitor and knockdown of Syk on the phosphorylation level of ERK and PKC. (A) Western blotting analysis of phosphorylation level of ERK, PKC and PKCα. MC3T3-E1 cells were cultured for 1 day. Then, cells were preincubated with the Syk inhibitor for 3 h. (B) Western blotting analysis of Syk knockdown in MC3T3-E1 cells by transfection with control or Syk (sites 1 and 2) siRNA. The cells transfected with siRNA were cultured for 48 h.

lymphatic systems. Recent findings have revealed that expression of Syk appears to be involved in a wide variety of cellular functions and in the pathogenesis of malignant cancers. As for bone metabolism, the roles of Syk in osteoclast differentiation and osteoclast function have been intensively studied thorough integrin αvβ3 activation and the M-CSF-DAP12-pathway. However, the role of Syk in osteoblastic differentiation has not been well elucidated and no reports have described the expression and effects of Syk on osteoblasts.

Our study showed the functions of Syk in osteoblastic differentiation for the first time. The present data can be summarized in two main results. First, inhibition of Syk promotes osteoblastic differentiation. Two different Syk inhibitors accelerated osteoblastic differentiation, appearing as increased ALP activity, ECM calcification and mRNA expression of ALP, OCN, Runx2, and Osterix in two different cell lines, M3CT3-E1 and ST2. In addition, knockdown of Syk increased gene expression of ALP, OCN, Runx2 in MC3T3-E1 cells. Expression of Osterix was increased with one siSyk, but decreased for the other siSyk. This might indicate that osteoblastic differentiation of Syk is unrelated to Osterix. Taken together, inhibition of Syk might stimulate osteoblastic differentiation in mesenchymal cells. Proliferation of MC3T3-E1 cells was decreased with high concentrations of Syk inhibitor, which might indicate that inhibition of Syk suppresses proliferation and promotes differentiation of osteoblasts. Second, MAPK and PKCα signal pathways might be involved in cellular signaling pathways of Syk in osteoblastic differentiation. Syk phosphorylates a variety of downstream targets, such as VAV family members, phospholipase Cγ (PLCγ) isoforms, regulatory subunits of phosphoinositide 3-kinase and SH2 domain-containing leukocyte protein [6,22]. These molecules probably participate in forming receptor-proximal signaling complexes and trigger downstream processes, including Ca^{2+} and PKC signaling, RAS homolog (Rho) family and protein tyrosine kinase 2-mediated cytoskeletal rearrangement, MAPK. Among these, we focused on MAPK and PKC, which are reportedly involved in osteoblastic differentiation. The role of MAPK activation in osteoblastic differentiation has been the subject of extensive investigation. MAPK activation has been reported to be required for osteoblastic differentiation by several investigators [23], whereas others have shown that MAPK activation inhibits osteoblastic differentiation [20,24]. We have reported that osteoblastic differentiation is suppressed by mitogen-activated protein kinase (MEK)-1 inhibition. Meanwhile, PKC plays an essential role in cellular signal transductions mediating a variety of biological functions [25–27]. Recent information from our laboratory has suggested that PKCα may play a pivotal role in cell signaling that modulates the differentiation and proliferation of osteoblasts and that PKCα suppresses osteoblastic differentiation [21]. Inhibition of Syk suppressed p42/44 MAPK phosphorylation in a dose-dependent manner. In addition to MAPK, inhibition of Syk suppressed PKC phosphorylation in a dose-dependent manner. In particular, PKCα phosphorylation was suppressed by Syk inhibition. We demonstrated that PKCβII was not expressed in MC3T3-E1 cells, as previously described. Our data thus suggest that phosphorylation of PKCα was coincidentally suppressed by Syk inhibition. These results are consistent with the functions of MAPK and PKCα on osteoblastic differentiation, which we have shown in the previous reports. Syk inhibition may thus promote osteoblastic differentiation through MAPK and PKCα.

Syk is also involved in inflammatory actions and Syk inhibitor has recently been developed for the treatment of inflammatory disease such as rheumatoid arthritis (RA) [28,29]. Syk regulates osteoclast development and function. In this study, we suggested that Syk inhibitor promoted osteoblastic differentiation. These findings indicate that Syk inhibitor could be developed for the treatment not only of RA, but also treatment of osteoporosis in both RA patients and non-RA patients.

In conclusion, the results of this study suggest that Syk might regulate osteoblastic differentiation and inhibition of this kinase could promote differentiation through MAPK and PKCα.

Conflict of interest

All authors have no conflicts of interest.

Acknowledgments

This work was partially supported by the Grant of The Nakatomi Foundation.

Appendix A. Supplementary data

Supplementary data associated with this article can be found, in the online version, at doi:10.1016/j.bbrc.2011.07.023.

References

[1] T. Taniguchi, T. Kobayashi, J. Kondo, K. Takahashi, H. Nakamura, J. Suzuki, K. Nagai, T. Yamada, S. Nakamura, H. Yamamura, Molecular cloning of a porcine gene syk that encodes a 72-kDa protein-tyrosine kinase showing high susceptibility to proteolysis, Journal of Biological Chemistry 266 (1991) 15790–15796.

[2] T. Kurosaki, M. Takata, Y. Yamanashi, T. Inazu, T. Taniguchi, T. Yamamoto, H. Yamamura, Syk activation by the Src-family tyrosine kinase in the B cell receptor signaling, Journal of Experimental Medicine 179 (1994) 1725–1729.

[3] S. Yanagi, T. Kurosaki, H. Yamamura, The structure and function of nonreceptor tyrosine kinase $p72^{syk}$ expressed in hematopoietic cells, Cellular Signalling 3 (1995) 185–193.

[4] A.M. Cheng, B. Rowley, W. Pao, A. Hayday, J.B. Bolen, T. Pawson, Syk tyrosine kinase required for mouse viability and B-cell development, Nature 378 (1995) 303–306.

[5] M. Turner, P.J. Mee, P.S. Costello, O. Williams, A.A. Price, L.P. Duddy, M.T. Furlong, R.L. Geahlen, V.L. Tyblewicz, Nature 378 (1995) 298–302.

[6] K. Sada, T. Takano, S. Yanagi, H. Yamamura, Structure and function of Syk protein-tyrosine kinase, Journal of Biochemistry 130 (2001) 177–186.

[7] G.A. Koretzky, F. Abtahian, M.A. Silverman, SLP76 and SLP65: complex regurelation of signaling in lymphocytes and beyond, Nature Review 6 (2006) 67–78.

[8] J. Schymeinsky, A. Sindrilaru, D. Frommhodl, M. Sperandio, T. Gerstl, C. Then, A. Mócsai, K. Scharffetter-Kochanek, B. Walzog, The Vav biding site of the non-receptor tyrosine kinase Syk at Try 348 is critical for beta2 integrin (CD11/CD18)-mediated neutrophil migration, Blood 108 (2006) 3919–3927.

[9] S. Johmura, M. Oh-hara, K. Inabe, Y. Nishikawa, K. Hayashi, E. Vigorito, D. Kitamura, M. Turner, K. Shingu, M. Hikida, T. Kurosaki, Regulation fo VAV localization in membrane rafts by adapter molecules Grb2 ad BLNK, Immunity 18 (2003) 777–787.

[10] T. Kurosaki, S.A. Johnson, L. Pao, K. Sada, H. Yamamura, J.C. Cambier, Role of the Syk autophosphorylation site and SH2 domains in B cell atigen receptor signaling, Journal of Experimental Medicine 1995 182 1815–1823.

[11] F. Kiefer, J. Brumell, N. Al-Alawi, S. Latour, A. Cheng, A. Veillete, S. Grinstein, T. Pawson, The Syk protein tyrosine kinase is essential for Fcgamma receptor signaling in macrophages and neutrophils, Molecular and Cellular Biology 18 (1998) 4209–4220.

[12] M.T. Crowley, P.S. Costello, C.J. Fitzer-Attas, M. Turner, F. Meng, C.A. Lowell, V.L. Tybulewicz, A.L. DeFranco, A critical role of Syk in signal transduction and phagocytosis mediated by Fcgamma receptors on macrophages, The Journal of experimental medicine 186 (1997) 1027–1039.

[13] J. Paloneva, M. Kestilä, J. Wu, A. Salminen, T. Böhling, V. Ruotsalainen, P. Hakola, A.B. Bakker, J.H. Phillips, P. Pekkarinen, L.L. Lanier, T. Timonen, L. Peltonen, Loss-of-function mutations in TYROBP (DAP12) result in a presenile dementia with bone cysts, Nature Genetics 25 (2000) 357–361.

[14] T. Kaifu, J. Nakahara, M. Inui, K. Mishima, T. Momiyama, M. Kaiji, A. Sugahara, H. Koito, A. Ujike-Asai, A. Nakamura, K. Kanazawa, K. Tan-Takeuchi, K. Iwasaki, W.M. Yokoyama, A. Kudo, M. Fujiwara, H. Asou, T. Takai, Osteopetrosis and thalamic hypomyelinosis with synaptic degeneration in DAP12-deficient mice, Journal of Clinical Investigation 111 (2003) 323–332.

[15] M.B. Humphrey, K. Ogasawara, W. Yao, S.C. Spusta, M.R. Daws, N.E. Lane, L.L. Lanier, M.C. Nakamura, The signaling adapter protein DAP12 regulates multinucleation during osteoclast development, Journal of Bone and Mineral Research 19 (2004) 224–234.

[16] A. Mósai, M.B. Humphrey, J.A. Van Ziffle, Y. Hu, A. Burghardt, S.C. Spusta, S. Majumdar, L.L. Lanier, C.A. Lowell, M.C. Nakamura, The immunomodulatory adapter proteins DAP12 and Fc receptor gamma-chain (Fc-Rgamma) regulate development of functional osteoclast thorough the Syk tyrosine kinase, Proceedings of the National Academy of Sciences of the United States of America 101 (2004) 6158–6163.

[17] T. Koga, M. Inui, K. Inoue, S. Kim, A. Suematsu, E. Kobayashi, T. Iwata, H. Ohnishi, T. Matozaki, T. Kodama, T. Taniguchi, H. Takayanagi, T. Takai, Costimulatory signals mediated by the ITAM motif cooperate with RANKL for bone hemeostasis, Nature 428 (2004) 758–763.

[18] W. Zou, H. Kitaura, J. Reeve, F. Long, V.L.J. Tybulewicz, S.J. Shattil, M.H. Ginsberg, F.P. Ross, S.L. Teitelbaum, Syk, c-Src, the αvβ3 integrin, and ITAM immunoreceptors, in concert, regulate osteoclastic bone resorption, Journal of Cell Biology 176 (2007) 877–888.

[19] R. Faccio, W. Zou, G. Colaianni, S.L. Teitelbaum, P. Ross, High dose M-CSF partially rescues the Dap12-/- osteoclast phenotype, Journal of Cellular Biochemistry 90 (2003) 871–883.

[20] C. Highchi, A. Myoui, N. Hashimoto, K. Kuriyama, K. Yoshida, H. Yoshidakawa, K. Itou, Continuous inhibiton of MAPK signalling promotes the early osteoblastic differentiation and mineralization of the extracellular matrix, Journal of Bone and Mineral Research 17 (2002) 1785–1794.

[21] A. Nakura, C. Highchi, K. Yoshida, H. Yoshikawa, PKCα suppresses osteoblastic differentiation, Bone 48 (2011) 476–481.

[22] A. Mósai, J. Ruland, V.L.J. Tybulewicz, The Syk tyrosine kinase: a crusial player in diverse biological functions, Nature Review. Immunology 10 (2010) 387–402.

[23] S. Gallea, F. Lallemand, A. Atfi, G. Rawadai, V. Ramez, S. Spinella-Jaegele, S. Kawai, C. Faucheu, L. Huet, R. Baron, S. Roman-Roman, Activation of mitogen-activated protein kinase cascades is involved in regulation of bone morphogenetic protein-2 induced osteoblast differentiation in pluripotent C2C12 cells, Bone 28 (2001) 491–498.

[24] A. Suzuki, J. Guicheux, G. Palmer, Y. Miura, Y. Oiso, J.P. Bonjour, J. Caverzasio, Exidence for a role of p38 MAP Kinase in expression of alkaline phosphatse during osteoblastic cell differentiation, Bone 30 (2002) 91–98.

[25] Y. Nishizuka, The role of protein kinase C in cell surface signal transduction and tumour promotion, Nature 308 (1984) 693–698.

[26] Y. Nishizuka, Turnover of inositol phospholipids and signal transduction, Science 225 (1984) 1365–1370.

[27] C. Keenan, D. Kelleher, Protein kinase C and the cytoskeleton, Cellular Signalling 10 (1998) 225–232.

[28] M. Bajpai, Fostamitinib, a Syk inhibitor prodrug for the treatment of inflammatory diseases, IDrugs 12 (2009) 174–185.

[29] Y.C. Lin, D.Y. Huang, C.L. Chu, W.W. Lin, Anti-inflammatory actions of Syk inhibitors in macrophages involve non-specific inhibitor of toll-like receptors-mediated JNK signaling pathway, Molecular Immunology 47 (2010) 1569–1578.